reactivity to other specific vasoactive agents is altered in hypertension (e.g., reactive oxygen species, nitric oxide, endothelin-1, etc.) and what region of the microcirculation is most susceptible to pathological changes (i.e., vessel branching generation and vessel size). Ultimately, it is anticipated that SR will provide an effective means of assessing potential therapeutic or prophylactic treatments for PAH.

In summary, we have demonstrated the effectiveness of SR for assessing changes in pulmonary blood flow distribution and functional changes (i.e., HPV) associated with the pathogenesis of PAH. Despite some limitations, the observations from this study can provide future direction for investigating the potential mechanisms responsible for these pathological changes. Of particular importance, future use of SR will provide an effective method for assessing the potential treatments for PAH.

ACKNOWLEDGMENTS

The SR experiments were performed at the BL28B2 in the SPring-8 with the approval of the Japan Synchrotron Radiation Research Institute (Proposal 2006BO464-NL2-NP).

GRANTS

This study was supported in part by the "Program for Promotion of Fundamental Studies in Health Sciences of the National Institute of Biomedical Innovation (NIBIO)" and also in part by a Grant-in-Aid for Scientific Research (16659210) and a Monash Synchrotron Fellowship (J. T. Pearson). We also acknowledge financial support from the access to Major Research Facilities Programme, which is a component of the International Science Linkages Programme (Australian Government).

REFERENCES

1. **Al-Tinawi A, Krenz GS, Rickaby DA, Linehan JH, Dawson CA.** Influence of hypoxia and serotonin on small pulmonary vessels. *J Appl Physiol* 76: 56–64, 1994.
2. **Archer S, Rich S.** Primary pulmonary hypertension: a vascular biology and translational research "Work in progress." *Circulation* 102: 2781–2791, 2000.
3. **Birnkrant DJ, Davis PB, Ernsberger P.** Visualization of high- and low-affinity β-adrenergic receptors in rat lung: upregulation by chronic hypoxia. *Am J Physiol Lung Cell Mol Physiol* 265: L389–L394, 1993.
4. **Chiong MA, Hatcher JD.** The sympathoadrenergic system in the cardiovascular responses to hypoxia in the dog. *Can J Physiol Pharmacol* 50: 674–683, 1972.
5. **Clini E, Cremona G, Campana M, Scotti C, Pagani M, Bianchi L, Giordano A, Ambrosino N.** Production of endogenous nitric oxide in chronic obstructive pulmonary disease and patients with cor pulmonale. Correlates with echo-Doppler assessment. *Am J Respir Crit Care Med* 162: 446–450, 2000.
6. **Diaz-Flores L, Gutierrez R, Varela H.** Angiogenesis: an update. *Histol Histopathol* 9: 807–843, 1994.
7. **Emery CJ, Bee D, Barer GR.** Mechanical properties and reactivity of vessels in isolated perfused lungs of chronically hypoxic rats. *Clin Sci (Lond)* 61: 569–580, 1981.
8. **Fried R, Reid LM.** Early recovery from hypoxic pulmonary hypertension: a structural and functional study. *J Appl Physiol* 57: 1247–1253, 1984.
9. **Hampl V, Archer SL, Nelson DP, Weir EK.** Chronic EDRF inhibition and hypoxia: effects on pulmonary circulation and systemic blood pressure. *J Appl Physiol* 75: 1748–1757, 1993.
10. **Hillier SC, Graham JA, Hanger CC, Godbey PS, Glenny RW, Wagner WWJ.** Hypoxic vasoconstriction in pulmonary arterioles and venules. *J Appl Physiol* 82: 1084–1090, 1997.
11. **Hislop A, Reid L.** New findings in pulmonary arteries of rats with hypoxia-induced pulmonary hypertension. *Br J Exp Pathol* 57: 542–554, 1976.
12. **Hislop A, Reid L.** Normal structure and dimensions of the pulmonary arteries in the rat. *J Anat* 125: 71–83, 1978.
13. **Hopkins N, McLoughlin P.** The structural basis of pulmonary hypertension in chronic lung disease: remodelling, rarefaction or angiogenesis? *J Anat* 201: 335–348, 2002.
14. **Howell K, Preston RJ, McLoughlin P.** Chronic hypoxia causes angiogenesis in addition to remodelling in the adult rat pulmonary circulation. *J Physiol* 547: 133–145, 2003.
15. **Huang KL, Wu CP, Kang BH, Lin YC.** Chronic hypoxia attenuates nitric oxide-dependent hemodynamic responses to acute hypoxia. *J Biomed Sci* 9: 206–212, 2002.
16. **Hyvelin J, Howell K, Nichol A, Costello CM, Preston RJ, McLoughlin P.** Inhibition of Rho-kinase attenuates hypoxia-induced angiogenesis in the pulmonary circulation. *Circ Res* 97: 185–191, 2005.
17. **Ikai A, Shirai M, Nishimura K, Ikeda T, Kameyama T, Ueyama K, Komeda M.** Maintenance of pulmonary vasculature tone by blood derived from the inferior vena cava in a rabbit model of cavopulmonary shunt. *J Thorac Cardiovasc Surg* 129: 199–206, 2005.
18. **Karamsetty VS, MacLean MR, McCulloch KM, Kane KA, Wadsworth RM.** Hypoxic constrictor response in the isolated pulmonary artery from chronically hypoxic rats. *Respir Physiol* 105: 85–93, 1996.
19. **Kelly DA, Hislop AA, Hall SM, Haworth SG.** Relationship between structural remodeling and reactivity in pulmonary resistance arteries from hypertensive piglets. *Pediatr Res* 58: 525–530, 2005.
20. **Kontos HA, Lower RR.** Role of β-adrenergic receptors in the circulatory response to hypoxia. *Am J Physiol* 217: 756–763, 1969.
21. **Le Cras TD, Markham NE, Tuder RM, Voelkel NF, Abman SH.** Treatment of newborn rats with a VEGF receptor inhibitor causes pulmonary hypertension and abnormal lung structure. *Am J Physiol Lung Cell Mol Physiol* 283: L555–L562, 2002.
22. **McMurtry IF, Petrun MD, Reeves JT.** Lungs from chronically hypoxic rats have decreased pressor response to acute hypoxia. *Am J Physiol Heart Circ Physiol* 235: H104–H109, 1978.
23. **Meyrick B, Fujiwara K, Reid L.** Smooth muscle myosin in precursor and mature smooth muscle cells in normal pulmonary arteries and the effect of hypoxia. *Exp Lung Res* 2: 303–313, 1981.
24. **Meyrick B, Hislop A, Reid L.** Pulmonary arteries of the normal rat: the thick walled oblique muscle segment. *J Anat* 125: 209–221, 1978.
25. **Meyrick B, Reid L.** The effect of continued hypoxia on rat pulmonary arterial circulation. An ultrastructural study. *Lab Invest* 38: 188–200, 1978.
26. **Moudgil R, Michelakis ED, Archer SL.** Hypoxic pulmonary vasoconstriction. *J Appl Physiol* 98: 390–403, 2005.
27. **Nagasaka Y, Bhattacharya J, Nanjo S, Gropper MA, Staub NC.** Micropuncture measurement of lung microvascular pressure profile during hypoxia in cats. *Circ Res* 54: 90–95, 1984.
28. **Patan S.** Vasculogenesis and angiogenesis. *Cancer Treat Res* 117: 3–32, 2004.
29. **Patan S, Munn LL, Tanda S, Roberge S, Jain RK, Jones RC.** Vascular morphogenesis and remodeling in a model of tissue repair: blood vessel formation and growth in the ovarian pedicle after ovariectomy. *Circ Res* 89: 723–731, 2001.
30. **Rabinovitch M, Gamble W, Nadas AS, Miettinen OS, Reid L.** Rat pulmonary circulation after chronic hypoxia: hemodynamic and structural features. *Am J Physiol Heart Circ Physiol* 236: H818–H827, 1979.
31. **Sasaki S, Kobayashi N, Dambara T, Kira S, Sakai T.** Structural organization of pulmonary arteries in the rat lung. *Anat Embryol (Berl)* 191: 477–489, 1995.
32. **Schwenke DO, Pearson JT, Kangawa K, Umetani K, Shirai M.** Imaging of the pulmonary circulation in the closed-chest rat using synchrotron radiation microangiography. *J Appl Physiol* 102: 787–793, 2007.
33. **Shirai M, Matsukawa K, Nishiura N, Kawaguchi AT, Ninomiya I.** Changes in efferent pulmonary sympathetic nerve activity during systemic hypoxia in anesthetized cats. *Am J Physiol Regul Integr Comp Physiol* 269: R1404–R1409, 1995.
34. **Shirai M, Shimouchi A, Kawaguchi AT, Sunagawa K, Ninomiya I.** Inhaled nitric oxide: diameter response patterns in feline small pulmonary arteries and veins. *Am J Physiol Heart Circ Physiol* 270: H974–H980, 1996.
35. **Shirai M, Shindo T, Ninomiya I.** β-Adrenergic mechanisms attenuated hypoxic pulmonary vasoconstriction during systemic hypoxia in cats. *Am J Physiol Heart Circ Physiol* 266: H1777–H1785, 1994.
36. **Tanaka A, Mori H, Tanaka E, Mohammed MU, Tanaka Y, Sekka T, Ito K, Shinozaki Y, Hyodo K, Ando M, Umetani K, Tanioka K, Kubota M, Abe S, Handa S, Nakazawa H.** Branching patterns of intramural coronary vessels determined by microangiography using synchrotron radiation. *Am J Physiol Heart Circ Physiol* 276: H2262–H2267, 1999.
37. **Tokiya R, Umetani K, Imai S, Yamashita T, Hiratsuka J, Imajo Y.** Observation of microvasculatures in athymic nude rat transplanted tumor

using synchrotron radiation microangiography system. *Acad Radiol* 11: 1039–1046, 2004.

38. **Weissmann N, Nollen M, Gerigk B, Ardeschir Ghofrani H, Schermuly RT, Gunther A, Quanz K, Fink L, Hanze J, Rose F, Seeger W, Grimminger F.** Downregulation of hypoxic vasoconstriction by chronic hypoxia in rabbits: effects of nitric oxide. *Am J Physiol Heart Circ Physiol* 284: H931–H938, 2003.
39. **Winter RJ, Dickinson KE, Rudd RM, Sever PS.** Tissue specific modulation of β-adrenoceptor number in rats with chronic hypoxia with an attenuated response to down-regulation by salbutamol. *Clin Sci (Lond)* 70: 159–165, 1986.
40. **Yamashita T, Kawashima S, Ozaki M, Namiki M, Shinohara M, Inoue N, Hirata K, Umetani K, Yokoyama M.** In vivo angiographic detection of vascular lesions in apolipoprotein E-knockout mice using a synchrotron radiation microangiography system. *Circ J* 66: 1057–1059, 2002.
41. **Zhao L, Crawley DE, Hughes JM, Evans TW, Winter RJ.** Endothelium-derived relaxing factor activity in rat lung during hypoxic pulmonary vascular remodeling. *J Appl Physiol* 74: 1061–1065, 1993.

nature medicine

Central control of bone remodeling by neuromedin U

Shingo Sato[1], Reiko Hanada[2], Ayako Kimura[1], Tomomi Abe[3], Takahiro Matsumoto[4,5], Makiko Iwasaki[1], Hiroyuki Inose[1], Takanori Ida[2], Michihiro Mieda[3], Yasuhiro Takeuchi[6], Seiji Fukumoto[7], Toshiro Fujita[7], Shigeaki Kato[4,5], Kenji Kangawa[8], Masayasu Kojima[2], Ken-ichi Shinomiya[1] & Shu Takeda[1]

Bone remodeling, the function affected in osteoporosis, the most common of bone diseases, comprises two phases: bone formation by matrix-producing osteoblasts[1] and bone resorption by osteoclasts[2]. The demonstration that the anorexigenic hormone leptin[3–5] inhibits bone formation through a hypothalamic relay[6,7] suggests that other molecules that affect energy metabolism in the hypothalamus could also modulate bone mass. Neuromedin U (NMU) is an anorexigenic neuropeptide that acts independently of leptin through poorly defined mechanisms[8,9]. Here we show that *Nmu*-deficient (*Nmu*$^{-/-}$) mice have high bone mass owing to an increase in bone formation; this is more prominent in male mice than female mice. Physiological and cell-based assays indicate that NMU acts in the central nervous system, rather than directly on bone cells, to regulate bone remodeling. Notably, leptin- or sympathetic nervous system–mediated inhibition of bone formation[6,7] was abolished in *Nmu*$^{-/-}$ mice, which show an altered bone expression of molecular clock genes (mediators of the inhibition of bone formation by leptin). Moreover, treatment of wild-type mice with a natural agonist for the NMU receptor decreased bone mass. Collectively, these results suggest that NMU may be the first central mediator of leptin-dependent regulation of bone mass identified to date. Given the existence of inhibitors and activators of NMU action[10], our results may influence the treatment of diseases involving low bone mass, such as osteoporosis.

Bone mass is maintained at a constant level between puberty and menopause by a succession of bone-resorption and bone-formation phases[11,12]. The discovery that neuronal control of bone remodeling is mediated by leptin[6] shed light on a new regulatory mechanism of bone remodeling and also suggested that bone mass may be regulated by a variety of neuropeptides[13]. In line with this observation, cannabinoids and pituitary hormones have been shown to be intimately involved in bone remodeling[14,15]. Leptin inhibits bone formation by binding to its receptors located in hypothalamus and thereby activating the sympathetic nervous system (SNS), which requires the adrenergic β2 receptors (Adrb2) expressed in osteoblasts[7,16]. Downstream of Adrb2, leptin signaling activates molecular clock genes that regulate osteoblast proliferation and hence bone formation[17]. In addition, leptin regulates bone resorption through two distinct pathways[16].

NMU is a small peptide produced by nerve cells in the submucosal and myenteric plexuses in the small intestine, and also by structures in the brain, including the dorsomedial nucleus of the hypothalamus[9]. It is generally assumed that NMU acts as a neuropeptide to regulate various aspects of physiology, including appetite, stress response and SNS activation[9]. Indeed, NMU-deficient (*Nmu*$^{-/-}$) mice develop obesity due to increased food intake and reduced locomotor activity that is believed, at least in part, to be leptin independent[8]. In addition, expression of NMU is diminished in leptin-deficient (*Lep*^{ob}) mice[18], but can be induced in these mice by leptin treatment[19]. In search of additional neuropeptides that regulate bone remodeling, we analyzed *Nmu*$^{-/-}$ mice.

When assessed at 3 and 6 months of age, both male and female *Nmu*$^{-/-}$ mice showed a high bone mass phenotype as compared to the wild type (WT), with male mice more severely affected than female mice (**Fig. 1a** and data not shown). The presence of a uniform increase in bone mineral density (BMD) along the femurs of *Nmu*$^{-/-}$ mice suggested that both trabecular and cortical bone were equally affected (**Supplementary Fig. 1** online). Microcomputed tomography analysis confirmed this observation (**Fig. 1b,c**). To determine whether this phenotype was secondary to the obesity of the *Nmu*$^{-/-}$ mice, we restricted their food intake for 1 month starting at 2 months of age. This manipulation normalized the body weight and serum insulin level of the *Nmu*$^{-/-}$ mice but did not affect their high bone mass phenotype (**Fig. 1d** and data not shown). Of note, when *Nmu*$^{-/-}$ mice were backcrossed to the C57BL/6J genetic background, their body weight became similar to that of their WT littermates; however, their BMD remained high (data not shown). These results suggest that NMU regulates bone mass independently of its regulation of energy metabolism, just as leptin does[7]. To better characterize the cellular nature of the bone phenotype in the *Nmu*$^{-/-}$ mice, we

[1]Department of Orthopaedic Surgery, Graduate School, 21st Century Center of Excellence Program, Tokyo Medical and Dental University, 1-5-45 Yushima, Bunkyo-ku, Tokyo 113-8519, Japan. [2]Division of Molecular Genetics, Institute of Life Science, Kurume University, 1-1 Hyakunen-kohen, Kurume, Fukuoka 839-0842, Japan. [3]Department of Molecular Neuroscience, Tokyo Medical and Dental University 1-5-45 Yushima, Bunkyo-ku, Tokyo 113-8519, Japan. [4]Institute of Molecular and Cellular Biosciences, University of Tokyo, 1-1-1 Yayoi, Bunkyo-ku, Tokyo 113-0032, Japan. [5]Exploratory Research for Advanced Technology, Japan Science and Technology Agency, 4-1-8 Honcho, Kawaguchi, Saitama 332-0012, Japan. [6]Toranomon Hospital Endocrine Center, 2-2-2 Toranomon, Minato-ku, Tokyo 105-8470, Japan. [7]Division of Nephrology and Endocrinology, Department of Internal Medicine, University of Tokyo Hospital, 7-3-1 Hongo, Bunkyo-ku, Tokyo 113-8655, Japan. [8]Department of Biochemistry, National Cardiovascular Center Research Institute, 5-7-1 Fujishiro-dai, Suita-shi, Osaka 565-8565, Japan. Correspondence should be addressed to S.T. (shu-tky@umin.ac.jp).

Received 4 June; accepted 8 August; published online 16 September 2007; doi:10.1038/nm1640

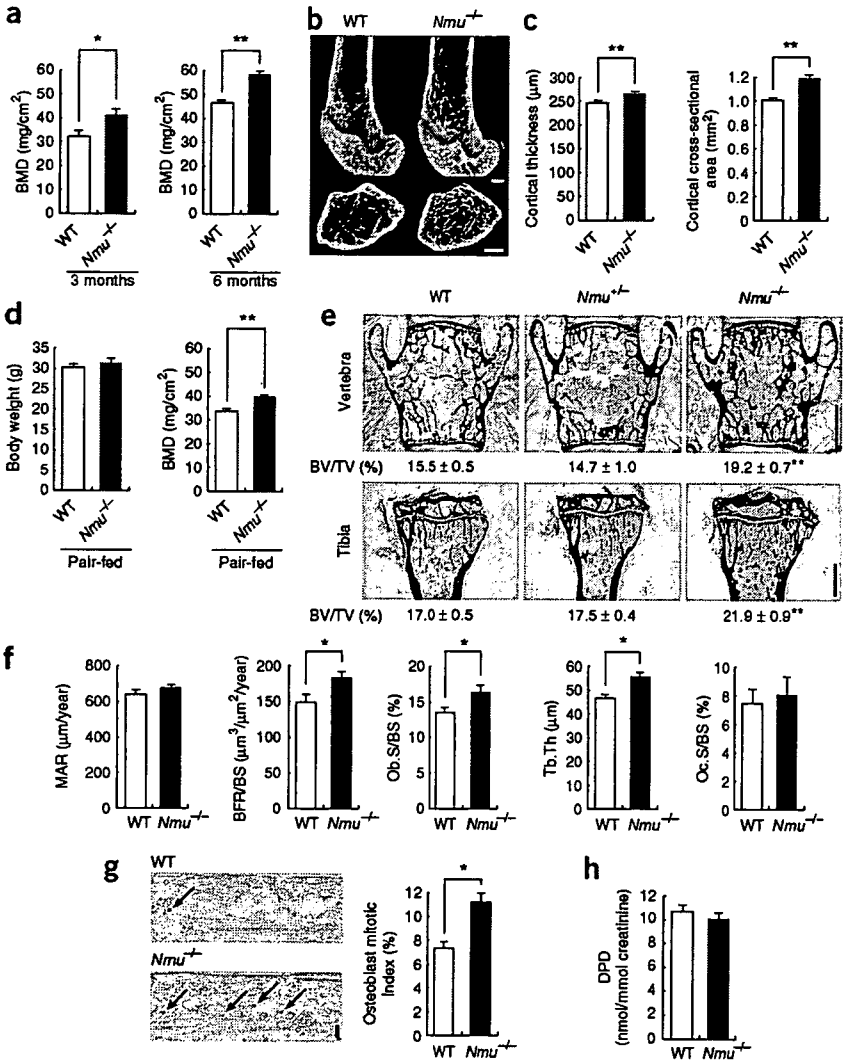

Figure 1 High bone mass in *Nmu*$^{-/-}$ mice due to increased bone formation. (**a**) Bone mineral density (BMD) of the femurs of 3 (left)- and 6 (right)-month-old male wild-type (WT) and *Nmu*$^{-/-}$ mice. (**b**) Micro-computed tomography (μCT) analysis of the distal femurs of male mice at 3 months. Scale bars, 500 μm. (**c**) Cortical thickness and cross-sectional area of the femurs of 3-month-old male mice. (**d**) Body weight and BMD of 3-month-old male mice with restricted food intake. (**e**) Histological analysis of the vertebrae and tibiae of 3-month-old male WT, *Nmu*$^{+/-}$ and *Nmu*$^{-/-}$ mice. Bone volume per tissue volume (BV/TV). Scale bars, 1 mm. (**f**) Histomorphometric analysis of the vertebrae of 3-month-old male mice. Mineral apposition rate (MAR), bone formation rate over bone surface area (BFR/BS), osteoblast surface area over bone surface area (Ob.S/BS), trabecular thickness (Tb. Th) and osteoclast surface area over bone surface area (Oc.S/BS). (**g**) Increased osteoblast proliferation in newborn *Nmu*$^{-/-}$ mice. Immunolocalization of BrdU incorporation (arrows) in the calvariae of WT and *Nmu*$^{-/-}$ mice (left). Osteoblast mitotic index (right). Scale bar, 20 μm. (**h**) Urinary elimination of deoxypyridinoline (DPD) in WT and *Nmu*$^{-/-}$ mice. **, $P < 0.01$; *, $P < 0.05$.

performed histological and histomorphometric analyses of vertebrae and tibiae in both male and female animals (**Fig. 1e** and **Supplementary Fig. 1**). At 3 and 6 months of age, *Nmu*$^{-/-}$ mice showed greater bone volume in both vertebrae and tibiae than did WT littermates, with male mice having a more pronounced phenotype (**Fig. 1e** and **Supplementary Fig. 1**). At the present time we do not have a clear explanation of the difference in phenotype severity between male and female mice. Bone formation rates (WT mice, 146.9 ± 12.3, *Nmu*$^{-/-}$ mice, 183.7 ± 10.3, $P < 0.05$) and osteoblast numbers were both significantly greater in the vertebrae and tibiae of *Nmu*$^{-/-}$ mice (**Fig. 1f** and **Supplementary Fig. 1**). The higher osteoblast numbers in the presence of a normal mineral apposition rate (**Fig. 1f** and **Supplementary Fig. 1**), which reflects the function of individual osteoblasts[20], suggested that osteoblast proliferation may be increased in *Nmu*$^{-/-}$ mice. Indeed, 5-bromo-2-deoxyuridine (BrdU)-positive proliferative osteoblast counts were significantly increased in *Nmu*$^{-/-}$ mice *in vivo* (**Fig. 1g**), demonstrating that NMU affects osteoblast proliferation. In contrast, *Nmu*$^{-/-}$ and WT mice showed comparable osteoclast numbers and osteoclast surface areas (**Fig. 1f** and **Supplementary Fig. 1**), suggesting that NMU does not affect bone resorption. This observation was further supported by the normal level of urinary elimination of deoxypyridinoline in *Nmu*$^{-/-}$ mice (**Fig. 1h**).

Taken together, these results demonstrate that NMU deficiency results in an isolated increase in bone formation leading to high bone mass. *Nmu*-heterozygote mice did not have an overt bone abnormality at any age analyzed (**Fig. 1e**).

Two cognate G protein–coupled receptors have been reported to be NMU receptors: NMUR1, which is expressed in various tissues, including the small intestine and lung (data not shown), and NMUR2, which is predominantly expressed in the hypothalamus and the small intestine (**Fig. 2a**)[18]. Both receptors and NMU itself were barely detectable in bone (**Fig. 2a**). To further exclude the possibility of a direct action of NMU on osteoblasts, we treated mouse primary osteoblasts with varying concentrations of NMU. Alkaline phosphatase activity, mineralization and expression of osteoblastic genes were all unaffected by this treatment (**Fig. 2b,c**). In addition, there were no differences between WT mice and *Nmu*$^{-/-}$ mice in the expression of osteoblastic genes *in vivo* (**Fig. 2d**). Moreover, both WT and *Nmu*$^{-/-}$ osteoblasts proliferated normally *in vitro* in response to NMU treatment (**Fig. 2e**), though *Nmu*$^{-/-}$ osteoblasts proliferated more than WT osteoblasts *in vivo* (**Fig. 1g**). Osteoclastic differentiation from bone marrow macrophages was unchanged by NMU treatment (**Fig. 2f**), as expected from the absence of a bone resorption defect *in vivo* (**Fig. 1f,h**). Taken together, these results strongly suggest that NMU's effect on bone may not come from its direct action on osteoblasts, but rather through another relay.

Because the anorexigenic effect of NMU requires a hypothalamic relay[8,19] and because hypothalamic neurons have been shown to regulate bone mass, we tested whether NMU's regulation of bone formation could involve a central relay. Continuous intracerebroventricular (i.c.v.) infusion of NMU into *Nmu*$^{-/-}$ mice decreased their fat mass and fat pad weight significantly, although body weight was not

affected (**Fig. 2g** and **Supplementary Fig. 2** online). In addition, NMU i.c.v. infusion eliminated the high bone mass phenotype in *Nmu*$^{-/-}$ mice (**Fig. 2g** and **Supplementary Fig. 2**), suggesting that NMU inhibits bone formation through the central nervous system.

The central nature of bone remodeling regulation by NMU, along with the notion that the anorexigenic effect of NMU may be independent of leptin[8], prompted us to examine whether leptin could be involved in the regulation of bone formation by NMU. To address this question, we performed i.c.v. infusion of NMU or leptin in *Lep*^{ob} mice. NMU decreased fat pad weight significantly, albeit to a milder extent than that achieved by leptin (**Fig. 3a** and **Supplementary Fig. 3** online). Body weight was not significantly changed by the NMU infusion, indicating that this treatment had only a mild effect on energy metabolism (data not shown). In contrast, NMU decreased bone mass in *Lep*^{ob} mice as efficiently as leptin did (**Fig. 3a**). These results indicate that NMU inhibits bone formation in a leptin-independent manner. Next, we asked whether leptin could correct the high bone mass phenotype of *Nmu*$^{-/-}$ mice. Leptin i.c.v. infusion decreased bone volume and bone formation in WT mice, as previously reported (**Fig. 3b** and **Supplementary Fig. 3**)[6]. However, the leptin paradoxically increased bone volume and osteoblast number in *Nmu*$^{-/-}$ mice (**Fig. 3b,c** and **Supplementary Fig. 3**). The fact that leptin decreased fat mass and fat pad weight in *Nmu*$^{-/-}$ mice and increased urinary elimination of normetanephrine, a metabolite of noradrenaline[17], verified that the administration of leptin was properly performed (**Fig. 3b,d** and **Supplementary Fig. 3**). Therefore, taken together, these results suggest that NMU acts downstream of leptin to regulate bone formation.

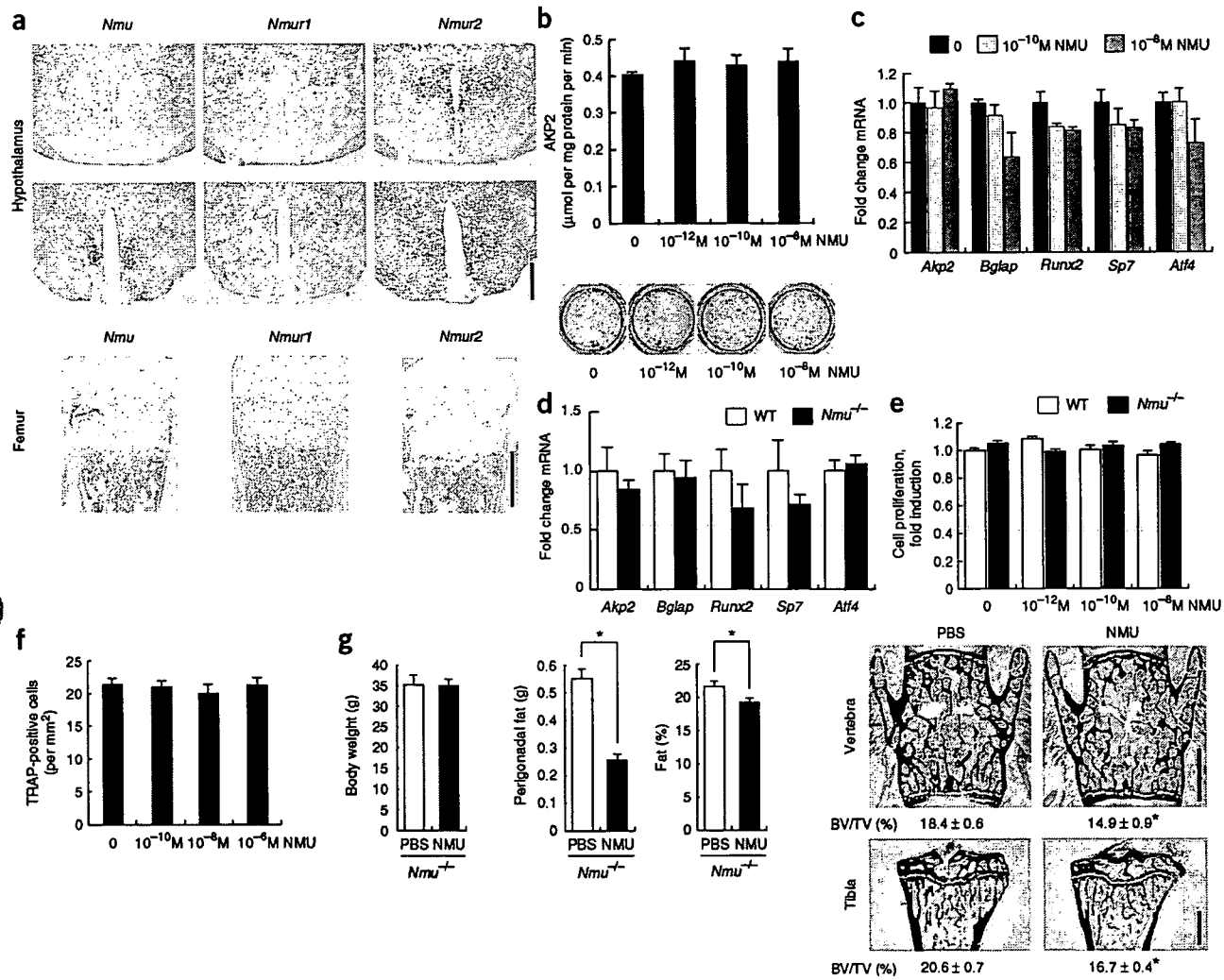

Figure 2 Absence of NMU's direct effect on osteoblasts; decrease in bone mass by NMU i.c.v. infusion. (**a**) Expression of *Nmu*, *Nmur1* and *Nmur2* in the hypothalamus at the atlas-levels of 38 (top) and 43 (bottom) and in the femur as shown by *in situ* hybridization. Note the expression of *Nmu* in the dorsomedial nucleus of the hypothalamus (DMH) (bottom) and *Nmur2* in paraventricular nucleus (top), arcuate nucleus and DMH (bottom). Scale bars, 500 μm. (**b–d**) Effect of NMU on osteoblast differentiation. (**b,c**) WT osteoblasts treated with NMU. (**b**) Alkaline phosphatase (AKP2) activity (top), mineralized nodule formation (bottom). (**c**) Expression of osteoblastic genes (*Akp2*, *Bglap*, *Runx2*, *Sp7* and *Atf4*), depicted as fold change over WT expression. (**d**) Expression of osteoblastic genes in WT and *Nmu*$^{-/-}$ femurs. (**e**) Effect of NMU on osteoblast proliferation. WT or *Nmu*$^{-/-}$ osteoblasts treated with NMU. (**f**) Effect of NMU on osteoclast differentiation. Bone marrow–derived osteoclasts treated with NMU. (**g**) Effect of NMU i.c.v. infusion on body weight, fat pad weight (perigonadal fat) and fat mass (left). Histological analysis of the vertebrae (top right) and tibiae (bottom right). Male mice at 3 months of age were used. Scale bars, 1 mm. *, $P < 0.05$.

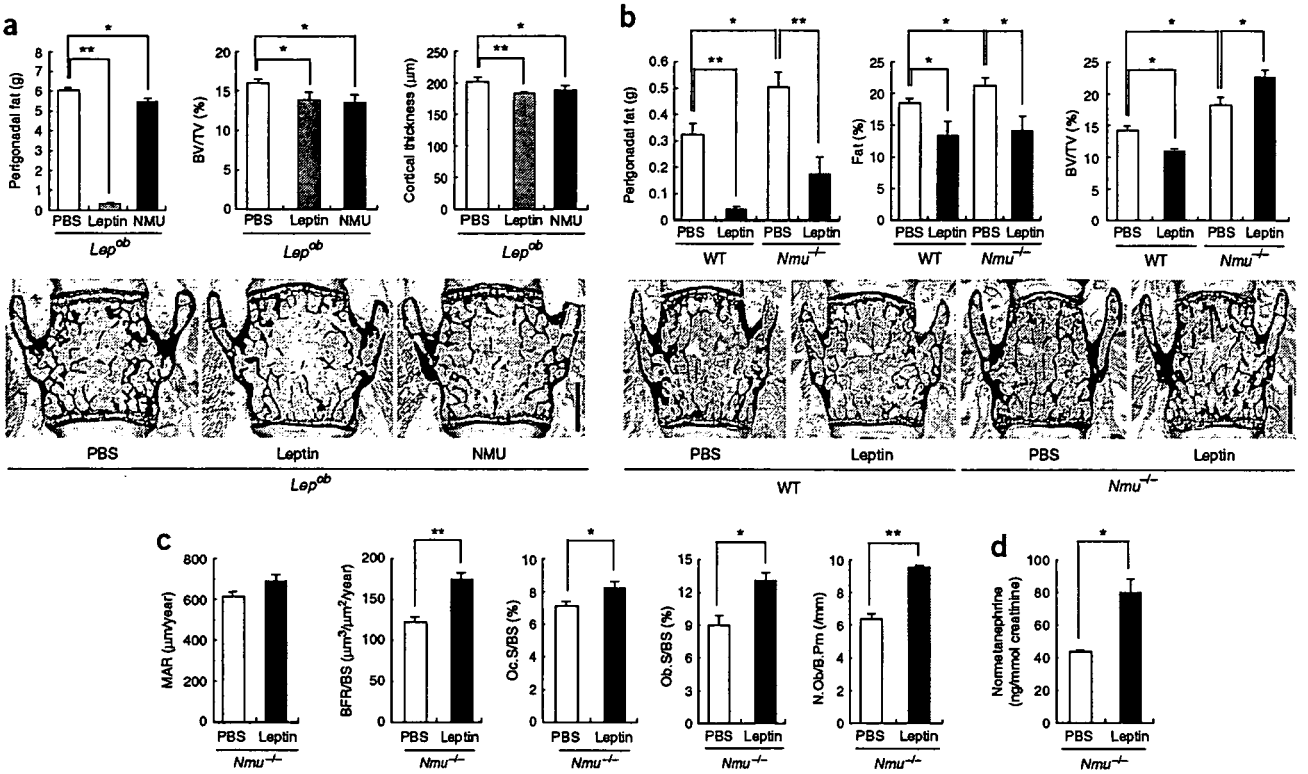

Figure 3 Leptin does not eliminate high bone mass in *Nmu*$^{-/-}$ mice. (**a**) Effect of NMU or leptin i.c.v. infusion in *Lep*^{ob} mice (3-month-old males). Fat pad weight and bone mass were determined by histology and cortical thickness by μCT analysis. (**b–d**) Effect of leptin i.c.v. infusion on *Nmu*$^{-/-}$ mice (3-month-old males). (**b**) Fat pad weight, fat mass and bone mass shown by histology. (**c**) Histomorphometric analysis. N. Ob/B.Pm indicates the number of osteoblasts per bone perimeter. (**d**) Urinary elimination of normetanephrine. Scale bars, 1 mm. **, $P < 0.01$; *, $P < 0.05$.

The SNS is a major mediator of leptin's antiosteogenic action[7]. NMUR2 is expressed in paraventricular nuclei, whose neurons directly project to the sympathetic preganglionic neurons, and NMU stimulates sympathetic outflow[9,21]. These observations, along with the fact that *Nmu*$^{-/-}$ mice have osteoblastic defects similar to the one observed in *Adrb2*-deficient mice[16], prompted us to explore whether NMU and sympathetic tone are in the same pathway regulating bone formation. Indeed, *Nmu/Adrb2* double heterozygote mice had higher bone mass than *Adrb2* single heterozygote mice (**Fig. 4a**), although *Nmu* single heterozygote mice had normal bone mass (**Fig. 1e** and **Supplementary Fig. 1**). Given that *Nmu* expression in the hypothalamus was reduced in *Nmu* single heterozygote mice (data not shown), compound heterozygosity of *Nmu* and *Adrb2* may have resulted in higher bone mass. Furthermore, this result suggests that these two pathways share a common molecule. Of note, *Nmu*$^{-/-}$ mice had a higher degree of urinary elimination of normetanephrine than WT littermates (**Fig. 4b**), which would decrease bone mass, yet they had high bone mass. This suggests that their high bone mass phenotype is not caused by decreased SNS activity, but is instead the result of resistance to the antiosteogenic activity of the SNS. This is in agreement with the observation that i.c.v. infusion of leptin, a potent stimulator of SNS activity, did not decrease bone mass in *Nmu*$^{-/-}$ mice (**Fig. 3b** and **Supplementary Fig. 3**). Furthermore, injection of isoproterenol, a sympathomimetic, reduced bone mass in WT mice[7] but not in *Nmu*$^{-/-}$ mice (**Fig. 4c** and **Supplementary Fig. 4** online). Thus, *Nmu*$^{-/-}$ mice are resistant to the antiosteogenic effects of both leptin and the SNS.

We present six experimental arguments to strongly suggest that the failure of leptin or isoproterenol to decrease bone mass in *Nmu*$^{-/-}$ mice is not due to leptin-SNS signaling defects. First, leptin infusion decreased fat pad weight equally well in WT and in *Nmu*$^{-/-}$ mice and could increase normetanephrine abundance in *Nmu*$^{-/-}$ mice (**Fig. 3b,d** and **Supplementary Fig. 3**). Second, the expression of *Adrb2* was not different in WT and *Nmu*$^{-/-}$ bones (**Fig. 4d**). Third, treatment with NMU did not affect *Adrb2* expression in osteoblasts (**Supplementary Fig. 5** online). Fourth, isoproterenol induced expression of *Tnfsf11* (encoding tumor necrosis factor superfamily, member 11) and decreased expression of *Tnfrsf11b* (encoding tumor necrosis factor superfamily, member 11b, also known as osteoprotegerin), *Runx2* (encoding runt-related transcription factor-2) and *Col1a1* (encoding collagen type I), molecular markers for the effect of SNS activation on osteoblasts, in both WT and *Nmu*$^{-/-}$ osteoblasts (**Fig. 4d**). Fifth, isoproterenol induced cAMP production equally well in WT and *Nmu*$^{-/-}$ osteoblasts (**Fig. 4e**). Sixth, and most notably, leptin increased bone resorption to a similar extent in WT and *Nmu*$^{-/-}$ mice (**Fig. 3c** and **Supplementary Fig. 3**).

The fact that the leptin-SNS pathway is intact in *Nmu*$^{-/-}$ mice, together with the paradoxical increase in osteoblast number induced by leptin i.c.v. infusion in *Nmu*$^{-/-}$ mice (**Fig. 3c**), suggests that NMU affects only the negative regulator of bone remodeling by leptin, that is, the molecular clock. Indeed, the expression of *Per1* and *Per2* (encoding period homolog-1 and -2, respectively) was downregulated in *Nmu*$^{-/-}$ bones as compared to WT bones (**Fig. 4f** and **Supplementary Fig. 6** online). Thus, NMU, acting through the central nervous system, affects the molecular clock in bone.

Because bone resorption in *Nmu*$^{-/-}$ mice was comparable to that in the wild type, despite the high SNS activity in these mice, we also

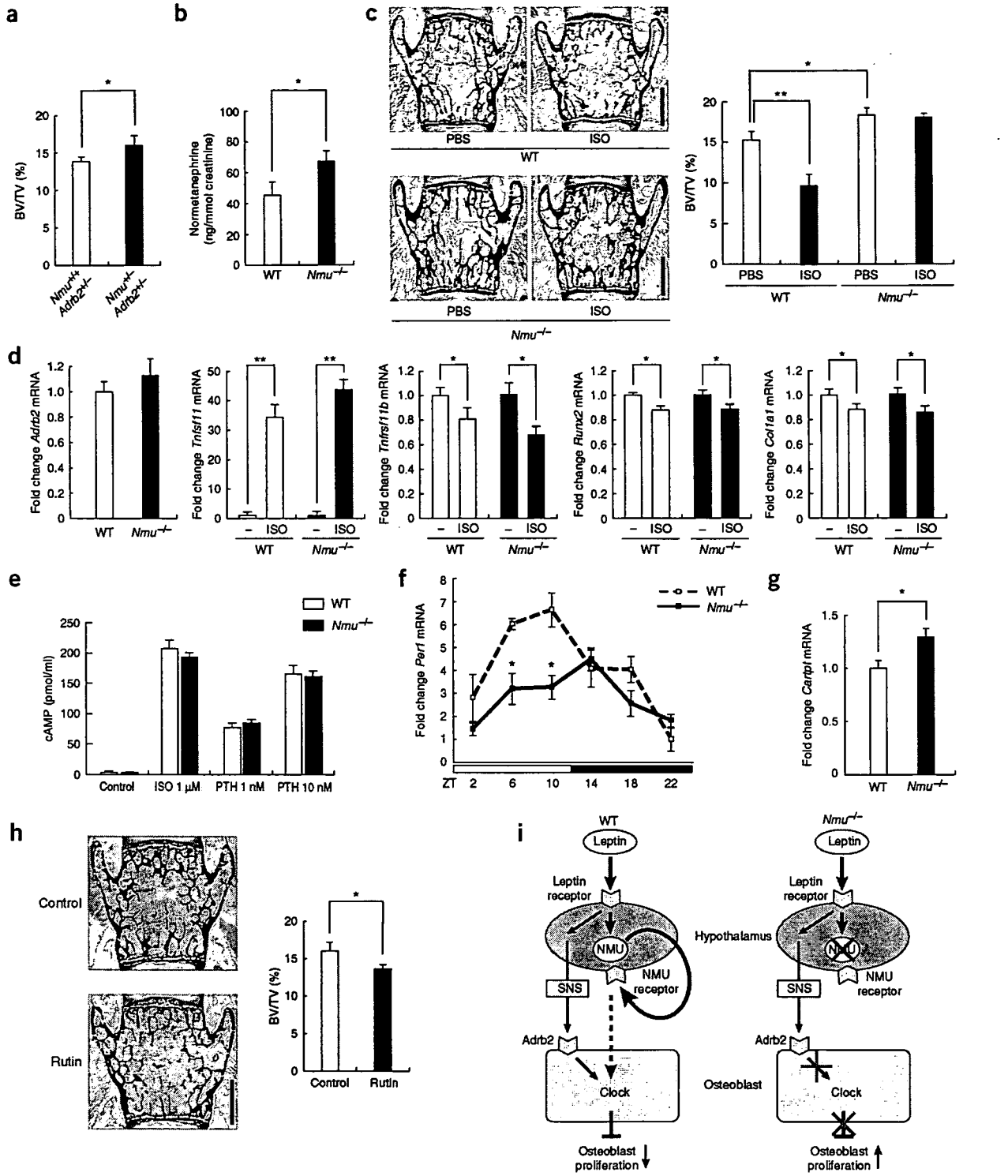

Figure 4 Sympathetic activation does not rescue high bone mass in *Nmu*$^{-/-}$ mice. (**a**) Bone mass in *Adrb2*$^{+/-}$/*Nmu*$^{+/+}$and *Adrb2*$^{+/-}$/*Nmu*$^{+/+}$ mice as determined by histology (3-month-old males). (**b**) Increased urinary elimination of normetanephrine in *Nmu*$^{-/-}$ mice. (**c**) Effect of sympathetic activation by isoproterenol (ISO) injection in *Nmu*$^{-/-}$ mice (3-month-old males). Shown is the bone mass of vertebrae as determined by histology. (**d**) Expression of *Adrb2* in the femurs of WT and *Nmu*$^{-/-}$ mice (left). Gene expression changes induced by isoproterenol (ISO) treatment of WT and Nmu$^{-/-}$ osteoblasts (four rightmost graphs). (**e**) cAMP concentration in the culture medium of WT and *Nmu*$^{-/-}$ osteoblasts after ISO treatment. Parathyroid hormone (PTH) was used as a control. (**f**) Expression of *Per1* in the femurs of WT and *Nmu*$^{-/-}$ mice. Zeitberger time (ZT) is indicated on the *x*-axis. (**g**) Expression of *Cartpt* in the hypothalamus of WT and *Nmu*$^{-/-}$ mice. (**h**) Rutin decreases bone mass in WT mice as determined by histological analysis of vertebrae (left) and quantitative histomorphometric analysis (right) (3-month-old males). Scale bar, 1 mm. **, $P < 0.01$; *, $P < 0.05$. (**i**) Model of leptin, sympathetic nervous system (SNS) and NMU signaling for the regulation of bone formation in WT mice (left) and *Nmu*$^{-/-}$ mice (right).

tested whether the expression of *Cartpt* (encoding cocaine- and amphetamine-regulated transcript propeptide), a central mediator of leptin's action on bone resorption[16], was altered in these mice. Indeed, *Cartpt* expression was increased in $Nmu^{-/-}$ mice as compared to WT littermates (**Fig. 4g** and **Supplementary Fig. 7** online). These results suggest that the protective activity of Cart on bone resorption compensates for the bone-resorbing activity induced by the SNS in $Nmu^{-/-}$ mice. The effect of other leptin-regulated neuropeptides, such as NPY (neuropeptide Y), AgRP (agouti-related protein) and α-MSH (α-melanotropin), will be limited, because the expression of *Npy* and *Agrp* was unchanged in $Nmu^{-/-}$ mice[8] and melanocortin 4 receptor, a major receptor for α-MSH, has been shown to have little effect on bone remodeling by itself[22].

Lastly, we treated WT mice with rutin, a natural NMUR2 agonist found in daily foods such as buckwheat[23]. Consistent with the high bone mass phenotype of the $Nmu^{-/-}$ mice, rutin decreased bone mass significantly in WT mice (**Fig. 4h**). This result, together with the predominant expression of *Nmur2* in the hypothalamus (**Fig. 2a**), suggests that NMU regulates bone remodeling through NMUR2.

Collectively, these results suggest that NMU, through a central relay and via an unidentified pathway, acts as a modulator of leptin-SNS-Adrb2 regulation of bone formation (**Fig. 4i**). However, one concern still remains: because leptin affects several pathways originating in the hypothalamus and elsewhere in the brain, i.c.v. infusion of leptin may have resulted in an uncoordinated change in leptin-regulated bone remodeling that does not reflect a physiological role of leptin. To rigorously address that question, an analysis of a mouse model in which a specific nucleus of the hypothalamus is activated by leptin will be necessary. From a therapeutic point of view, given the lack of an obesity phenotype in *Nmur2*-deficient mice[24], an NMU antagonist may be a candidate for the treatment of bone-loss disorders without inducing unwanted body weight gain.

METHODS

Animals. $Nmu^{-/-}$ and $Adrb2^{-/-}$ mice were previously described[8,16]. We purchased C57BL/6J mice and C57BL/6J Lep^{ob} from the Jackson Laboratory. We maintained all of the mice under a 12 hr light-dark cycle with *ad libitum* access to regular food and water, unless specified. For pair-fed experiments, we caged $Nmu^{-/-}$ and WT mice individually for 12 weeks as described[8]. In brief, $Nmu^{-/-}$ mice were given access to water *ad libitum* and fed the amount of chow eaten on the previous day by a WT littermate. We determined mouse genotypes by PCR as previously described[8,16]. We injected isoproterenol (10 mg/kg, Sigma) intraperitoneally (i.p.) once daily for 4 weeks. Rutin (Sigma) was administered orally 300 mg per kg body weight per day for 4 weeks. All animal experiments were performed with the approval of the Animal Study Committee of Tokyo Medical and Dental University and conformed to relevant guidelines and laws.

Dual X-ray absorptiometry and microcomputed tomography analysis. We measured bone mineral density (BMD) of the femurs and fat pad composition by DCS-600 (Aloka). We obtained two-dimensional images of the distal femurs by microcomputed tomography (μCT, Comscan). We measured cortical thickness and cross-sectional area at the center of the femur. We examined at least eight mice for each group.

Histological and histomorphometric analysis. We injected calcein (25 mg/kg, Sigma) i.p. 5 and 2 d before sacrifice. We stained undecalcified sections of the third and fourth lumbar vertebrae and tibiae with von Kossa staining. We performed static and dynamic histomorphometric analyses using the Osteomeasure Analysis System (Osteometrics). We analyzed 8–10 mice for each group.

***In situ* hybridization analysis.** We performed *in situ* hybridization analysis according to the established protocol[25]. Antisense cRNA probe for *Cartpt* was previously described[26]. We used fragments of cDNA for *Nmu* (105 base pairs upstream to 647 base pairs downstream of the initiation codon), *Nmur1* (13–1242 base pairs downstream of the initiation codon) and *Nmur2* (16–1252 base pairs downstream of the initiation codon) to generate antisense probes. We stained sections hybridized with ^{35}S-labeled probes with Hoechst 33528 and quantitatively analyzed the expression of *Cartpt* with a phosphorimager (Bass–2500, Fuji). The atlas-level of designations corresponds to those described previously[27]. We analyzed six mice for each group.

Measurement of deoxypyridinoline cross-links and normetanephrine. We measured urinary deoxypyridinoline cross-links (DPD) and normetanephrine with the METRA DPD-EIA kit (Quidel) and the Normetanephrine-ELISA kit (ALPCO), respectively, according to the manufacturer's instructions. We used creatinine values to standardize between samples (Creatinine Assay Kit, Cayman). We examined eight samples for each group.

Cell culture. *In vitro* primary osteoblast cultures were established as previously described[6]. Briefly, we cultured primary osteoblasts from calvariae of 4-d-old mice in α-MEM (Sigma) containing ascorbic acid (0.1 mg/ml, Sigma). We added NMU to the medium twice daily. After 14 d, we measured alkaline phosphatase activity with the ALP kit (Wako). For the mineralization assay, we supplemented the medium with β-glycerophosphate (5 mM, Sigma). We assessed mineralized nodule formation by von Kossa staining. We performed the cell proliferation and cAMP assays with the Cell Proliferation Assay (Promega) and cAMP EIA kit (Cayman Chemical), respectively. *In vitro* osteoclast differentiation has been described previously[16]. Briefly, bone marrow cells of 2-month-old mice were cultured in the presence of human macrophage colony-stimulating factor (10 ng/ml, R&D Systems) for 2 d and then differentiated into osteoclasts with human RANKL (50 ng/ml, Peprotech) and human macrophage colony-stimulating factor (10 ng/ml) for 3 d. We counted tartrate-resistant acid phosphatase (TRAP)-positive multinucleated cells (more than 3 nuclei). We performed all the cell cultures in triplicate or quadruplicate wells and repeated more than 3 times.

BrdU immunohistochemistry. For BrdU labeling, we injected 100 μg BrdU i.p. into 3-d-old mice 1 h before sacrifice. We embedded calvariae in paraffin and cut coronally. We detected BrdU-incorporated osteoblasts with the BrdU Immunohistochemistry Kit (Exalpha Biologicals). We calculated the number of BrdU-positive osteoblasts over the total number of osteoblasts (osteoblast mitotic index) at three different locations (+3.0, 3.5 and 4.0 AP (0 point: bregma)) per mouse. We analyzed six mice per group.

Intracerebroventricular infusion. Intracerebroventricular infusion was performed as previously described[6]. Briefly, we exposed the calvaria of an anesthetized mouse, implanted a 28-gauge cannula (Plastics ONE) into the third ventricle and then connected the cannula to an osmotic pump (Durect) placed in the dorsal subcutaneous space of the mouse. We infused rat Neuromedin U-23 (Peptide Institute) or human leptin (Sigma) at 0.125 nmol/hr or 8 ng/hr, respectively, for 28 d.

Quantitative RT-PCR analysis. After flushing mouse bone marrow out of the bone with PBS, we extracted bone RNA with Trizol (Invitrogen) and performed reverse transcription for cDNA synthesis. We performed quantitative analysis of gene expression with the Mx3000P real-time PCR system (Stratagene). Primer sequences are available upon request. We used GAPDH expression as an internal control.

Statistical analysis. All data are represented as mean ± s.d. ($n = 8$ or more). We performed statistical analysis by Student's *t*-test. Values were considered statistically significant at $P < 0.05$. Results are representative of more than four individual experiments.

Note: Supplementary information is available on the Nature Medicine website.

ACKNOWLEDGMENTS

We thank G. Karsenty, M. Patel and P. Ducy for critical review of the manuscript and for helpful discussions; K. Nakao, M. Noda, T. Matsumoto and S. Ito for insightful suggestions; P. Barrett (Rowett Research Institute, UK) for providing a plasmid for the *Cartpt* probe; and J. Chen, M. Starbuck, S. Sunamura, H. Murayama, H. Yamato, and M. Kajiwara for technical assistance. This work was supported by grant-in-aid for scientific research from the Japan Society for

the Promotion of Science, a grant for the 21st Century Center of Excellence program from the Ministry of Education, Culture, Sports, Science, and Technology of Japan, Ono Medical Research Foundation, Yamanouchi Foundation for Research on Metabolic Disorders, Kanae Foundation for the Promotion of the Medical Science and the Program for Promotion of Fundamental Studies in Health Sciences of the National Institute of Biomedical Innovation of Japan.

AUTHOR CONTRIBUTIONS

S. Sato conducted most of the experiments. K. Kangawa and M. Kojima generated *Nmu*$^{-/-}$ mice. R. Hanada and T. Ida conducted *in vitro* experiments. S. Fukumoto, Y. Takeuchi and T. Fujita contributed by conducting dual X-ray absorptiometry analyses and providing suggestions on the project. M. Iwasaki prepared the constructs. A. Kimura performed i.c.v. infusion experiments. H. Inose conducted μCT analyses. T. Matsumoto and S. Kato conducted histological analyses for brain tissue. T. Abe and M. Mieda performed *in situ* hybridization analysis. S. Takeda and K. Shinomiya designed the project. S. Takeda supervised the project and wrote most of the manuscript.

Published online at http://www.nature.com/naturemedicine
Reprints and permissions information is available online at http://npg.nature.com/reprintsandpermissions

1. Rodan, G.A. & Martin, T.J. Therapeutic approaches to bone diseases. *Science* **289**, 1508–1514 (2000).
2. Teitelbaum, S.L. & Ross, F.P. Genetic regulation of osteoclast development and function. *Nat. Rev. Genet.* **4**, 638–649 (2003).
3. Saper, C.B., Chou, T.C. & Elmquist, J.K. The need to feed: homeostatic and hedonic control of eating. *Neuron* **36**, 199–211 (2002).
4. Ahima, R.S. & Flier, J.S. Leptin. *Annu. Rev. Physiol.* **62**, 413–437 (2000).
5. Spiegelman, B.M. & Flier, J.S. Obesity and the regulation of energy balance. *Cell* **104**, 531–543 (2001).
6. Ducy, P. *et al.* Leptin inhibits bone formation through a hypothalamic relay: a central control of bone mass. *Cell* **100**, 197–207 (2000).
7. Takeda, S. *et al.* Leptin regulates bone formation via the sympathetic nervous system. *Cell* **111**, 305–317 (2002).
8. Hanada, R. *et al.* Neuromedin U has a novel anorexigenic effect independent of the leptin signaling pathway. *Nat. Med.* **10**, 1067–1073 (2004).
9. Brighton, P.J., Szekeres, P.G. & Willars, G.B. Neuromedin U and its receptors: structure, function, and physiological roles. *Pharmacol. Rev.* **56**, 231–248 (2004).
10. Fang, L., Zhang, M., Li, C., Dong, S. & Hu, Y. Chemical genetic analysis reveals the effects of NMU2R on the expression of peptide hormones. *Neurosci. Lett.* **404**, 148–153 (2006).
11. Riggs, B.L., Khosla, S. & Melton, L.J. 3rd. A unitary model for involutional osteoporosis: estrogen deficiency causes both type I and type II osteoporosis in postmenopausal women and contributes to bone loss in aging men. *J. Bone Miner. Res.* **13**, 763–773 (1998).
12. Karsenty, G. & Wagner, E.F. Reaching a genetic and molecular understanding of skeletal development. *Dev. Cell* **2**, 389–406 (2002).
13. Harada, S. & Rodan, G.A. Control of osteoblast function and regulation of bone mass. *Nature* **423**, 349–355 (2003).
14. Idris, A.I. *et al.* Regulation of bone mass, bone loss and osteoclast activity by cannabinoid receptors. *Nat. Med.* **11**, 774–779 (2005).
15. Abe, E. *et al.* TSH is a negative regulator of skeletal remodeling. *Cell* **115**, 151–162 (2003).
16. Elefteriou, F. *et al.* Leptin regulation of bone resorption by the sympathetic nervous system and CART. *Nature* **434**, 514–520 (2005).
17. Fu, L., Patel, M.S., Bradley, A., Wagner, E.F. & Karsenty, G. The molecular clock mediates leptin-regulated bone formation. *Cell* **122**, 803–815 (2005).
18. Howard, A.D. *et al.* Identification of receptors for neuromedin U and its role in feeding. *Nature* **406**, 70–74 (2000).
19. Wren, A.M. *et al.* Hypothalamic actions of neuromedin U. *Endocrinology* **143**, 4227–4234 (2002).
20. Parfitt, A.M. The physiological and clinical significance of bone histomorphometric data. in *Bone Histomorphometry* (ed. Recker, R.R.) 143–223 (CRC Press, Boca Raton, FL, 1983).
21. Chu, C. *et al.* Cardiovascular actions of central neuromedin U in conscious rats. *Regul. Pept.* **105**, 29–34 (2002).
22. Ahn, J.D., Dubern, B., Lubrano-Berthelier, C., Clement, K. & Karsenty, G. Cart overexpression is the only identifiable cause of high bone mass in melanocortin 4 receptor deficiency. *Endocrinology* **147**, 3196–3202 (2006).
23. Kalinova, J., Triska, J. & Vrchotova, N. Distribution of vitamin E, squalene, epicatechin, and rutin in common buckwheat plants (*Fagopyrum esculentum* Moench). *J. Agric. Food Chem.* **54**, 5330–5335 (2006).
24. Zeng, H. *et al.* Neuromedin U receptor 2–deficient mice display differential responses in sensory perception, stress, and feeding. *Mol. Cell. Biol.* **26**, 9352–9363 (2006).
25. Elias, C.F. *et al.* Leptin differentially regulates NPY and POMC neurons projecting to the lateral hypothalamic area. *Neuron* **23**, 775–786 (1999).
26. Graham, E.S. *et al.* Neuromedin U and Neuromedin U receptor-2 expression in the mouse and rat hypothalamus: effects of nutritional status. *J. Neurochem.* **87**, 1165–1173 (2003).
27. Paxinos, G. & Franklin, K. *The Mouse Brain in Stereotaxic Coordinates* 2nd edn. (Academic Press, San Diego, 2001).

Available online at www.sciencedirect.com
ScienceDirect
Regulatory Peptides 145 (2008) 37–41
REGULATORY PEPTIDES
www.elsevier.com/locate/regpep

Identification and functional analysis of a novel ligand for G protein-coupled receptor, Neuromedin S

Mikiya Miyazato [a,*], Kenji Mori [a], Takanori Ida [b], Masayasu Kojima [b], Noboru Murakami [c], Kenji Kangawa [a]

[a] Department of Biochemistry, National Cardiovascular Center Research Institute, Fujishirodai, Suita, Osaka 565-8565, Japan
[b] Division of Molecular Genetics, Institute of Life Science, Kurume University, Kurume, Fukuoka 839-0861, Japan
[c] Department of Veterinary Physiology, Faculty of Agriculture, University of Miyazaki, Miyazaki 889-2192, Japan

Available online 24 August 2007

Abstract

We identified a novel 36-amino acid neuropeptide in rat brain as an endogenous ligand for the G protein-coupled receptors FM-3/GPR66 and FM-4/TGR-1, which were identified to date as the neuromedin U (NMU) receptors, and designated this peptide neuromedin S (NMS) because it was specifically expressed in the suprachiasmatic nucleus (SCN) of the hypothalamus. NMS shared a C-terminal core structure with NMU. NMS mRNA was highly expressed in the central nervous system, spleen and testis. In rat brain, NMS expression was restricted to the ventrolateral portion of the SCN and has a diurnal peak under light/dark cycling, but remains stable under constant darkness. Intracerebroventricular (ICV) administration of NMS in rats induced nonphotic type phase shifts in the circadian rhythm of locomotor activity. ICV injection of NMS also decreased 12-h food intake during the dark period in rats. This anorexigenic effect was more potent than that observed with the same dose of NMU. ICV administration of NMS increased proopiomelanocortin (POMC) mRNA expression in the arcuate nucleus (Arc) and corticotropin-releasing hormone mRNA in the paraventricular nucleus, and induced c-Fos expression in the POMC neurons in the Arc. These findings suggest that NMS is implicated in the regulation of circadian rhythm and feeding behavior.

Keywords: Neuromedin S; G protein-coupled receptor; FM-3/GPR66; FM-4/TGR-1; Circadian rhythm; Feeding

1. Introduction

The progress of human genome sequencing has revealed the existence of several hundred orphan G protein-coupled receptors (GPCRs), for which ligands have not yet been identified [1]. GPCRs play crucial roles in cell-to-cell communication involved in a variety of physiological phenomena, and are the most common target of pharmaceutical drugs. Therefore, identification of endogenous ligands for orphan GPCRs will lead to clarification of novel regulatory mechanisms of physiological phenomena and to novel drug targets.

Neuromedin U (NMU), originally isolated from porcine spinal cord, is a brain–gut peptide that has potent contractile activity on uterine smooth muscle [2]. The peripheral activities of NMU include smooth muscle contraction, blood pressure elevation and modification of intestinal ion transport, whereas centrally, NMU suppresses feeding and induces the release of stress-mediating molecules such as adrenocorticotropic hormone and corticosterone [2–8]. In previous studies, two orphan GPCRs, FM-3/GPR66 and FM-4/TGR-1, were identified as NMU receptor type-1 (NMU1R) and type-2 (NMU2R), respectively [5,6,9,10].

Recently, we identified a novel 36-amino acid neuropeptide in rat brain as another endogenous ligand for FM-3/GPR66 and FM-4/TGR-1 using a reverse-pharmacological technique [11]. This neuropeptide was designated neuromedin S (NMS), because it is specifically expressed in the suprachiasmatic nucleus (SCN) in the brain. The SCN is the site of the master circadian pacemaker in mammals and important for the regulation of energy balance [12–15]. NMS was suggested to be involved in circadian oscillation systems and feeding regulation [11,16].

* Corresponding author. Tel.: +81 6 6833 5012; fax: +81 6 6835 5402.
E-mail address: miyazato@ri.ncvc.go.jp (M. Miyazato).

0167-0115/$ - see front matter © 2007 Elsevier B.V. All rights reserved.
doi:10.1016/j.regpep.2007.08.013

2. Purification of NMS

To search for the endogenous ligands of the orphan GPCR FM-4/TGR-1 (identified to date as NMU2R), we constructed a CHO cell line stably expressing FM-4/TGR-1. Using this cell line, we measured the increase in the intracellular calcium ion concentration ($[Ca^{2+}]_i$) induced by peptide extracts prepared from rat small intestine and brain as described previously [6,17]. Gel filtration of small intestinal extracts revealed one group of fractions capable of increasing $[Ca^{2+}]_i$ in CHO cells expressing FM-4/TGR-1, and NMU was isolated from these fractions (Fig. 1A). On the other hand, two groups of fractions were found in brain extracts. One group of fractions co-eluted with the one found in the small intestine, and another one eluted in fractions with a larger molecular mass (~4000), indicating that the rat brain contains another endogenous ligand for FM-4/TGR-1 (Fig. 1B). Therefore, this activity was purified to homogeneity by five successive steps of HPLC (Fig. 1C). The final yield of the purified peptide was approximately 2.5 pmol from 420 rat brains (510 g).

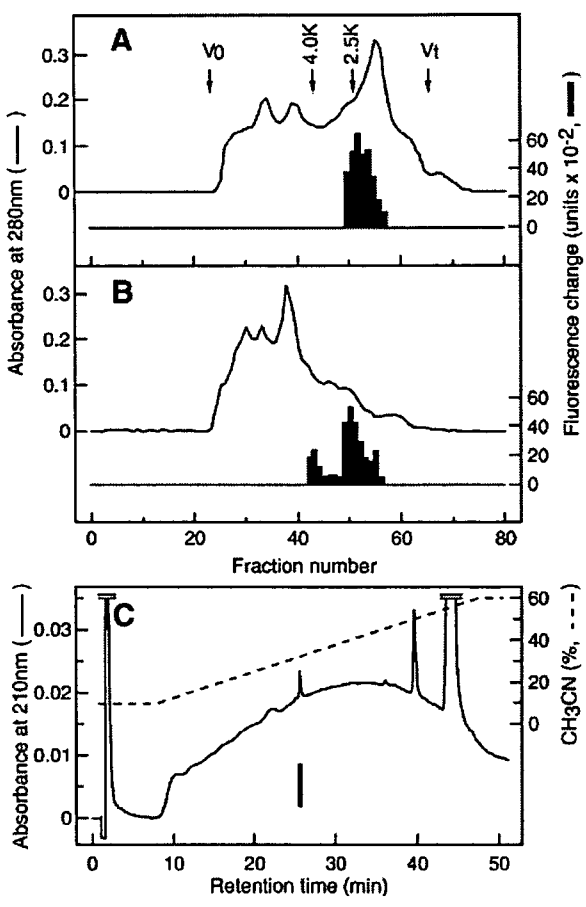

Fig. 1. Purification of NMS. (A, B) Gel filtration on a Sephadex G-50 column of basic peptide fractions from rat small intestine (A) and brain (B). Black bars indicate fluorescence change due to $[Ca^{2+}]_i$ increase in CHO cells expressing FM-4/TGR-1. Vo, void volume; Vt, total volume. Column: Sephadex G-50 (fine), 2.9×145 cm. Eluent: 1 M CH_3COOH. Fraction size: 15 ml/tube. (C) Final purification of NMS by reverse phase-HPLC. Black bar indicates $[Ca^{2+}]_i$-increasing activity. Column: Chemcosorb 3ODS-H, 2.1×75 mm (Chemco). Flow rate: 0.2 ml/min. Solvent system: a linear gradient elution from (a) to (b) for 40 min. H_2O:CH_3CN:10% TFA for (a) was 90:10:1, for (b) 40:60:1 (v/v).

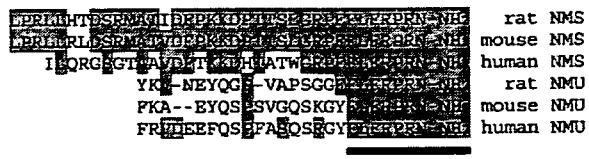

Fig. 2. Sequence comparison of NMS and NMU. Rat, mouse and human NMS and NMU sequences are aligned. Residues identical between peptides are shaded. Conserved core sequences are indicated by a solid underline.

3. Structure determination of NMS

The purified peptide was subjected to sequence analysis by a protein sequencer, giving the following partial N-terminal amino acid sequence: LPRLLHTDSRMATIDFPKK. To elucidate the complete amino acid sequence of NMS, rat, mouse and human cDNAs encoding NMS were isolated from the brain of each species [11]. Rat prepro-NMS was a 152-residue protein containing four potential processing sites. The N-terminal sequence of NMS directly followed the third processing site, indicating that NMS is generated by cleavage at the third and fourth sites. The fourth processing site contained glycine, which presumably serves as an amide donor for C-terminal amidation. We therefore deduced the primary structure of NMS to be a C-terminally amidated 36-residue peptide. Mass-spectrometric analysis revealed that the observed monoisotopic *m/z* value of the purified peptide (4240.2) was very close to the theoretically predicted value for rat NMS (4240.3). The N-terminal portion of NMS has no sequence homology to previously known peptides or proteins. On the other hand, the C-terminally amidated seven-residue sequence of NMS is identical to that of NMU (Fig. 2); this sequence has been found to be essential for NMU receptor binding [2]. Because NMS and NMU share a core structure that is required for binding to receptors, the interaction of NMS with FM-3/GPR66 and FM-4/TGR-1 was examined. NMS and NMU showed comparable potency and efficacy for both receptors, and showed similar affinity to FM-3/TGR-1. On the other hand, NMS had a higher affinity to FM-4/TGR-1 than did NMU [11]. These data indicated that NMS, as well as NMU, is a cognate ligand for both FM-3/GPR66 and FM-4/TGR-1.

4. Tissue distribution of NMS mRNA

The tissue distribution of NMS mRNA in rats was investigated using quantitative RT-PCR. The expression of NMS mRNA was mainly found in the central nervous system, spleen and testis. In the brain, NMS mRNA was expressed predominantly in the SCN, with only very slight expression in other regions (Fig. 3A). It is reported that high levels of NMU mRNA were detected in the gastrointestinal tract and pituitary gland, and moderate levels of expression were observed in the central nervous system, thyroid gland, trachea, testis and ovary [9]. In the brain, NMU mRNA was expressed in the ventromedial hypothalamic regions (arcuate nucleus (Arc) and

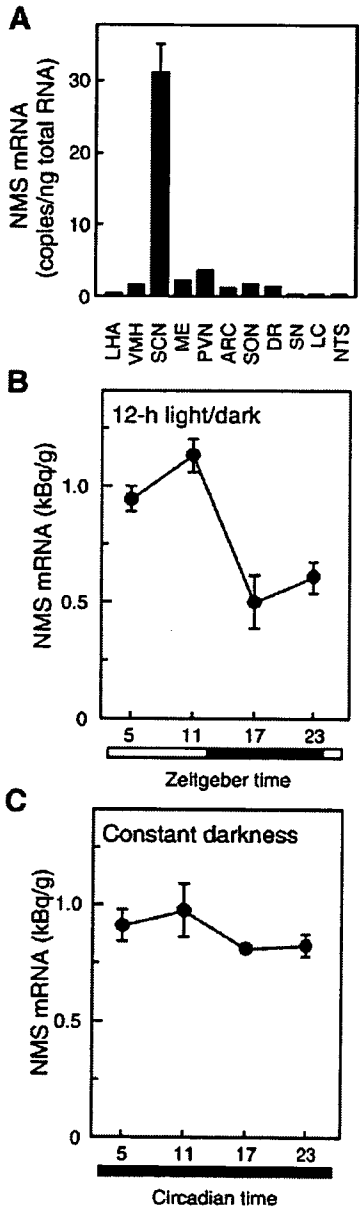

Fig. 3. Expression studies of rat NMS. (A) Quantitative RT-PCR analysis of NMS mRNA in rat brain regions. Each column represents the mean±s.e.m. of triplicate experiments. LHA, lateral hypothalamic area; VMH, ventromedial hypothalamus; SCN, suprachiasmatic nucleus; ME, median eminence; PVN, paraventricular nucleus; ARC, arcuate nucleus; SON, supraoptic nucleus; DR, dorsal raphe; SN, substantia nigra; LC, locus coeruleus; NTS, nucleus of the solitary tract. (B, C) Temporal expression profiles of NMS mRNA. Animals were maintained under 12-h light/dark cycles (B) or constant darkness for two days (C). The amount of NMS mRNA was quantified by *in situ* hybridization analysis. Data represent the means±s.e.m. of 3–4 animals. Open and filled horizontal bars indicate light and dark periods, respectively.

median eminence) and caudal brainstem [5]. *In situ* hybridization histochemistry, as well as RT-PCR analysis, showed that the NMS mRNA expression was restricted to the SCN in rat brain [11]. The SCN is divided into the ventrolateral portion, where the neuropeptide vasoactive intestinal polypeptide (VIP) is expressed, and the dorsomedial portion, where the neuropeptide arginine vasopressin is expressed [18]. NMS mRNA was expressed in the ventrolateral SCN, in a similar manner to VIP mRNA [11].

5. Role of NMS in circadian oscillator system

The SCN is the site of the master circadian pacemaker in mammals, which governs the circadian rhythm of behavioral and physiological processes. We thus examined the time-dependent profile of the NMS mRNA expression in rat SCN. Under 12-h light/dark cycles, a pronounced rhythmic expression of NMS mRNA was observed, with the largest decrease occurring during the dark period, followed by a gradual increase until the late light period at ZT11 (Zeitgeber time, ZT; ZT0 is lights on and ZT12 is lights off) (Fig. 3B). Under conditions of constant darkness, no NMS mRNA oscillation was observed (Fig. 3C), indicating that the expression of NMS is not under the control of clock-gene families that generate circadian rhythm by an autoregulatory transcription/translation feedback loop [12,13,19]. These data suggest that NMS may be involved in the regulation of circadian rhythm upstream of the endogenous pacemaker.

To elucidate the role of NMS within the SCN, we examined the effect of ICV administration of NMS on the circadian rhythm of locomotor activity in rats maintained under constant darkness. When injected at CT2-9 (circadian time, CT; CT0-12 is subjective day and CT12-24 is night), 1 nmol of NMS phase-advanced the rhythm of locomotor activity, whereas administration at CT22-24 induced a phase delay (Fig. 4). The phase response curve (PRC) for NMS was very similar to that for nonphotic stimuli [20]. These data suggest that NMS is a candidate for a nonphotic entrainment factor of circadian rhythm.

We reported that ICV administration of NMU also induces phase shifts [21]. However, the magnitude of the phase-shift induced by NMU is smaller than that caused by NMS and the shapes of the NMS and NMU PRCs were subtly different [11,21]. Two types of receptors for NMS and NMU are expressed in the SCN and each mRNA has an intrinsic rhythmic expression with a different circadian pattern [21]. The difference in the PRC shapes for NMS and NMU may be due to the timing of receptor expression and different affinities of the receptors to the respective peptides in the CNS. It would be important to determine the

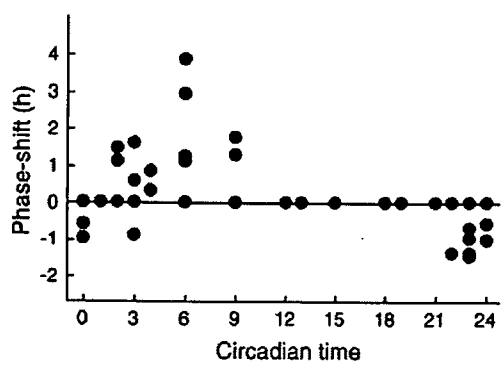

Fig. 4. Phase-response plot for ICV administration of 1 nmol NMS. The plus and minus values indicate phase advance and delay, respectively. $n=3$–5. The data points at CT12, 13, 15, 18, 19 and 21 overlap.

endogenous peptide/receptor pairs and their efficiencies to elucidate the functional roles of NMS and NMU in the circadian oscillator system of the SCN.

6. Role of NMS in feeding regulation

The SCN is involved in the organization of daily metabolic activity and the regulation of energy balance [14,15]. Because NMU is an anorexigenic neuropeptide involved in the central regulation of feeding behavior [5–7,9], NMS may also play a role in feeding regulation. ICV injection of NMS reduced 12-h food intake during the dark period in a dose-dependent manner (Fig. 5A). ICV injection of 3 nmol NMS and NMU into rats resulted in a significant decrease in 12-h food intake. On the other hand, at doses of 0.5 nmol and 1 nmol, only NMS injection suppressed food intake. To understand the molecular mechanisms involved in NMS-induced suppression of feeding, the expression of proopiomelanocortin (POMC) and corticotropin-releasing hormone (CRH) mRNA was investigated. ICV administration of NMS augmented the levels of POMC mRNA in the Arc and CRH mRNA in the paraventricular nucleus (PVN) (Fig. 5, B and C), and induced c-Fos expression in POMC neurons in the Arc (Fig. 5D). Pretreatment with both SHU9119 (an antagonist for α-melanocyte stimulating hormone (α-MSH)) and α-hCRF (an antagonist for CRH) attenuated NMS-induced suppression of food intake in a dose-dependent manner in fasted rats [16]. These results suggest that α-MSH in the Arc and CRH in the PVN are involved in NMS action on feeding.

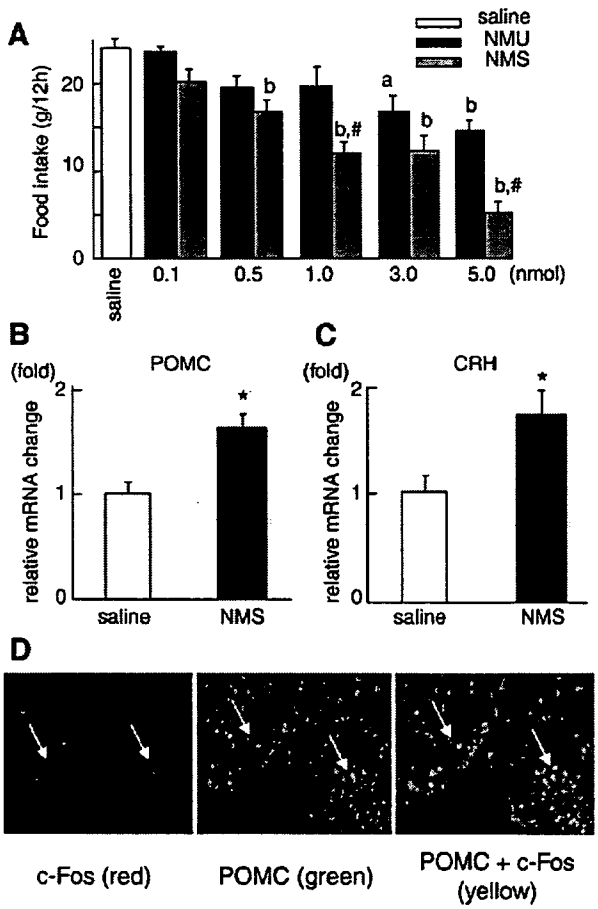

Fig. 5. Involvement of NMS in feeding. (A) Comparison of food intake during the dark period after ICV administration of NMS and NMU to rats (n=8–10 in each group). Each bar and vertical line represents the mean±s.e.m. Food intake of free-feeding rats was examined during a period of 12 h from 19:00 to 7:00. Each peptide was injected at 18:45 (a, $P<0.05$; b, $P<0.01$ *vs.* saline; #, $P<0.01$ *vs.* NMU at the same dose as NMS). (B, C) Quantitative RT-PCR on NMS administered rats (n=8 per group). ICV administration of NMS augmented the levels of POMC mRNA in the Arc (B) and CRH mRNA in the PVN (C). (*, $P<0.05$ *vs.* saline) (D) Induction of c-Fos protein in POMC cells within the Arc following ICV injection of NMS. Ninety min after ICV injection of 0.5 nmol NMS, brain was removed. Double immunostaining for c-Fos (red) and POMC (green) was performed. Each arrow indicates the example of immunoreactive cell. (For interpretation of the references to color in this figure legend, the reader is referred to the web version of this article).

7. Conclusion

We have identified a novel 36-residue neuropeptide NMS, which was purified from rat brain extracts. The restricted expression of NMS in the SCN and the ability of NMS to shift the phase of the circadian rhythm demonstrate that this newly identified peptide is important for the regulation of circadian rhythm. NMS is a candidate for a nonphotic entrainment factor of circadian rhythm. Furthermore, NMS was demonstrated to be an anorexigenic neuropeptide in rats. Both CRH and α-MSH may be involved in NMS-induced suppression of food intake. Further investigation of the function of NMS will help in our understanding of the regulatory mechanism of circadian rhythm and feeding behavior.

Acknowledgements

We thank Prof. Yoichi Ueta and Dr. Ryota Serino for their cooperation. This study was supported in part by grants-in-aid from the Ministry of Education, Culture, Sports, Science and Technology of Japan, and the Program for Promotion of Fundamental Studies in Health Sciences of the National Institute of Biomedical Innovation (NIBIO).

References

[1] Vassilatis DK, Hohmann JG, Zeng H, Li F, Ranchalis JE, Mortrud MT, Brown A, Rodriguez SS, Weller JR, Wright AC, Bergmann JE, Gaitanaris GA. The G protein-coupled receptor repertories of human and mouse. Proc Natl Acad Sci USA 2003;100:4903–8.

[2] Minamino N, Kangawa K, Matsuo H. Neuromedin U-8 and U-25: novel uterus stimulating and hypertensive peptides identified in porcine spinal cord. Biochem Biophys Res Commun 1985;130:1078–85.

[3] Chu C, Jin Q, Kunitake T, Kato K, Nabekura T, Nakazato M, Kangawa K, Kannan H. Cardiovascular actions of central neuromedin U in conscious rats. Regul Pept 2002;105:29–34.

[4] Brown DR, Quito FL. Neuromedin U octapeptide alters ion transport in porcine jejunum. Eur J Pharmacol 1988;155:159–62.

[5] Howard AD, Wang R, Pong SS, Mellin TN, Strack A, Guan XM, Zeng Z, Williams DL, Feighner SD, Nunes CN, Murphy B, Stair JN, Yu H, Jiang Q, Clements MK, Tan CP, McKee KK, Hreniuk DL, McDonald TP, Lynch KR, et al. Identification of receptors for neuromedin U and its role in feeding. Nature 2000;406:70–4.

[6] Kojima M, Haruno R, Nakazato M, Date Y, Murakami N, Hanada R, Matsuo H, Kangawa K. Purification and identification of neuromedin U as an endogenous ligand for an orphan receptor GPR66 (FM3). Biochem Biophys Res Commun 2000;276:435–8.
[7] Wren AM, Small CJ, Abbott CR, Jethwa PH, Kennedy AR, Murphy KG, Stanley SA, Zollner AN, Ghatei MA, Bloom SR. Hypothalamic actions of neuromedin U. Endocrinology 2002;143:4227–34.
[8] Hanada R, Nakazato M, Murakami N, Sakihara S, Yoshimatsu H, Toshinai K, Hanada T, Suda T, Kangawa K, Matsukura S. A role for neuromedin U in stress response. Biochem Biophys Res Commun 2001;289:225–8.
[9] Fujii R, Hosoya M, Fukusumi S, Kawamata Y, Habata Y, Hinuma S, Onda H, Nishimura O, Fujino M. Identification of neuromedin U as the cognate ligand of the orphan G protein-coupled receptor FM-3. J Biol Chem 2000;275:21068–74.
[10] Raddatz R, Wilson AE, Artymyshyn R, Bonini JA, Borowsky B, Boteju LW, Zhou S, Kouranova EV, Nagorny R, Guevarra MS, Dai M, Lerman GS, Vaysse PJ, Branchek TA, Gerald C, Forray C, Adham N. Identification and characterization of two neuromedin U receptors differentially expressed in peripheral tissues and the central nervous system. J Biol Chem 2000;275:32452–9.
[11] Mori K, Miyazato M, Ida T, Murakami N, Serino R, Ueta Y, Kojima M, Kangawa K. Identification of neuromedin S and its possible role in the mammalian circadian oscillator system. EMBO J 2005;24:325–35.
[12] Reppert SM, Weaver DR. Molecular analysis of mammalian circadian rhythms. Annu Rev Physiol 2001;63:647–76.
[13] Reppert SM, Weaver DR. Coordination of circadian timing in mammals. Nature 2002;418:935–41.
[14] la Fleur SE, Kalsbeek A, Wortel J, Fekkes ML, Buijs RM. A daily rhythm in glucose tolerance: a role for the suprachiasmatic nucleus. Diabetes 2001;50:1237–43.
[15] Kreier F, Yilmaz A, Kalsbeek A, Romijn JA, Sauerwein HP, Fliers E, Buijs RM. Hypothesis: shifting the equilibrium from activity to food leads to autonomic unbalance and the metabolic syndrome. Diabetes 2003;52:2652–6.
[16] Ida T, Mori K, Miyazato M, Egi Y, Abe S, Nakahara K, Nishihara M, Kangawa K, Murakami N. Neuromedin S is a novel anorexigenic hormone. Endocrinology 2005;146:4217–23.
[17] Kojima M, Hosoda H, Date Y, Nakazato M, Matsuo H, Kangawa K. Ghrelin is a growth-hormone-releasing acylated peptide from stomach. Nature 1999;402:656–60.
[18] Moore RY, Speh JC, Leak RK. Suprachiasmatic nucleus organization. Cell Tissue Res 2002;309:89–98.
[19] Lowrey PL, Takahashi JS. Genetics of the mammalian circadian system: photic entrainment, circadian pacemaker mechanisms, and posttranslational regulation. Annu Rev Genet 2000;34:533–62.
[20] Mrosovsky N. Locomotor activity and non-photic influences on circadian clocks. Biol Rev 1996;71:343–72.
[21] Nakahara K, Hanada R, Murakami N, Teranishi H, Ohgusu H, Fukushima N, Moriyama M, Ida T, Kangawa K, Kojima M. The gut–brain peptide neuromedin U is involved in the mammalian circadian oscillator system. Biochem Biophys Res Commun 2004;318:156–61.

Available online at www.sciencedirect.com
ScienceDirect
ELSEVIER
Biochemical and Biophysical Research Communications 361 (2007) 457–461
BBRC
www.elsevier.com/locate/ybbrc

Neuromedin S exerts an antidiuretic action in rats

Takumi Sakamoto [a], Kenji Mori [b], Keiko Nakahara [a], Mikiya Miyazato [b], Kenji Kangawa [b], Hiroshi Sameshima [c], Noboru Murakami [a,*]

[a] *Department of Veterinary Physiology, Faculty of Agriculture, University of Miyazaki, Miyazaki 889-2192, Japan*
[b] *Department of Biochemistry, National Cardiovascular Center Research Institute, Fujishirodai 5-7-1, Suita, Osaka 565-8565, Japan*
[c] *Department of Obstetrics and Gynecology, Faculty of Medicine, Miyazaki University, Miyazaki 889-2192, Japan*

Received 4 July 2007
Available online 18 July 2007

Abstract

We recently identified neuromedin S (NMS) as an endogenous ligand for the FM-4/TGR-1 receptor. Here, we examined the possible involvement of central NMS in regulation of urinary output and vasopressin (AVP) release in rats. Intracerebroventricular (icv) injection of NMS induced a dose-dependent increase in the plasma level of AVP, followed by a decrease of nocturnal urinary output. Expression of cFos after icv injection of NMS was observed in the supachiasmatic nucleus (SCN), arcuate nucleus, paraventricular nucleus (PVN), and supraoptic nucleus (SON). The cFos expressing cells in PVN and SON, but not SCN, were then double-stained using antibodies against the vasopressin. On the other hand, icv injection of neuromedin U, which also binds to the FM-4/TGR-1 receptor, required a concentration ten times higher than that of NMS in order to exert the same antidiuretic potency. These results suggest that central NMS may exert a physiological antidiuretic action via vasopressin release.

Keywords: Neuromedin S; Neuromedin U; Vasopressin; Antidiuretic action

In addition to neuromedin U, we have recently discovered the novel peptide neuromedin S (NMS) as an endogenous ligand for two orphan G-protein-coupled receptors, FM-3/GPR66 and FM-4/TGR-1, using a reverse-pharmacological technique [1]. FM-3/GPR66 and FM-4/TGR-1 had already been identified as neuromedin U receptor type-1 (NMUR1) and type-2 (NMUR2), respectively [2–4]. Rat NMS is a 36-amino acid neuropeptide that is specifically expressed in the suprachiasmatic nucleus (SCN) [1]. Although NMS shares a C-terminal core structure (7 amino acid residues) with NMU and activates both recombinant NMU1R and NMU2R expressed in Chinese hamster ovary cells, NMS is not a splice variant of neuromedin U, because both the NMS and neuromedin U genes have been mapped to discrete chromosomes. In addition, although neuromedin U mRNA has been detected in peripheral and central organs, the distribution of NMS is limited to the testis, spleen, and hypothalamus, especially the SCN [1–3]. NMS has been shown to have several physiological roles in rats, including involvement in circadian oscillation systems, since intracerebroventricular (icv) administration of NMS induces phase-dependent phase shifts in the circadian rhythm of locomotor activity in rats kept under constant darkness [1]. In addition, NMS may be involved in feeding regulation, because icv injection of NMS decreases food intake in a dose-dependent manner [5]. Recently, it has been shown that NMS regulate luteinizing hormone secretion [6].

NMUR1 is located in a wide range of peripheral tissues such as intestine, testis, pancreas, uterus, lung, and kidney. On the other hand, expression of NMUR2 is limited to areas of the central nervous system [2,3]. Therefore, NMS may have an unknown role in the central nervous system. We examined the expression of cFos after icv injection of

* Corresponding author. Fax: +81 985 58 7265.
E-mail address: a0d201u@cc.miyazaki-u.ac.jp (N. Murakami).

0006-291X/$ - see front matter © 2007 Elsevier Inc. All rights reserved.
doi:10.1016/j.bbrc.2007.07.036

NMS to search for the site of action of NMS in the central nervous system. When NMS was injected icv, cFos expression was observed specifically in the paraventricular nucleus (PVN), arcuate nucleus (Arc), supraoptic nucleus (SON), and SCN [5]. Although the expression of cFos in the PVN, Arc, and SCN may be related to its biological role in feeding regulation and circadian rhythm mentioned above, its physiological role in the SON is unknown.

On the other hand, the PVN and SON are known to be common sites synthesizing arginine–vasopressin (AVP) and oxytocin (OXT) [7,8]. Recently, NMU2R was detected in AVP-positive neurons in the PVN, indicating a possible role of NMS in the secretion of this hormone [9]. However, the relationship between NMS and AVP remains to be elucidated. AVP synthesized in the magnocellular region of the SON and PVN is exported to the posterior pituitary gland and secreted into the peripheral blood, subsequently acting on the kidney through specific receptors in the distal renal tubule to decrease urine volume. In the present study, we examined the possible involvement of central NMS in AVP secretion and urinary output in rats.

Materials and methods

Animals and icv injection. Male Wistar rats, weighing 300–350 g, were housed in individual Plexiglas cages in an animal room maintained under a constant light–dark cycle (lights on from 7:00 to 19:00 h) and temperature (22 ± 1 °C) for at least one week. Food and water were provided ad libitum. Icv cannulae were implanted into the lateral cerebral ventricles by a method that has been described previously [5]. After surgery, all rats were housed individually in Plexiglas cages. During a 6-day postoperative recovery period, the rats became accustomed to the handling procedure. Rat NMS or rat neuromedin U (Peptide Institute Inc., Osaka, Japan) was dissolved in saline, and 10 μl of the solution was injected into each free-moving rat through a 27-gauge injection cannula connected to a 50-μl Hamilton syringe. All procedures were performed in accordance with the Japan Physiological Society's guidelines for animal care.

Measurement of plasma AVP. Whole blood was collected by decapitation at 5, 60, and 180 min after icv injection of 0.02, 0.2, and 2 nmol NMS at 18:45 h into a tube containing EDTA and the proteinase inhibitor, Aprotinin (Sigma–Aldrich Inc.). Each group consisted of 8 rats. After centrifugation at 4 °C, the plasma was stored at −80 °C until measurement of AVP. AVP concentration was measured using an EIA kit (Assay designs Co., Ann Arbor, MI, USA) following the manufacturer's protocol.

Measurement of urinary volume and water intake. Before measurement, rats ($n = 4$/each group) were maintained individually in metabolic cages for four days to allow them to habituate. Twelve-hour urinary volume and water intake were measured every day in the dark phase, because each was very slight during the light period. After habituation, icv injection of 0.02, 0.2, and 2 nmol of NMS and neuromedin U was performed at 18:45 h, and then urinary volume and water intake were measured at 07:00 on the following morning. The control rats were injected with the same volume of saline. These experiments were repeated twice, and a total of 8 samples were collected in each group.

Immunohistochemistry for FM-4. Immunohistochemical analyses for the NMUR2 in the PVN and SON were performed using a modification of a method described previously [10]. The brain was placed in fixative for 5 days at 4 °C and then transferred to 0.1 M phosphate buffer containing 20% sucrose. Each brain was cut into serial, 18-μm-thick sections at −20 °C with a cryostat. The sections were incubated for 2 days with a rabbit anti-NMUR2 antibody (Abcam Ltd., Cambridge, UK) at 4 °C. Slides were then incubated with Alexa-546-labeled goat-anti-rabbit IgG antibody (Molecular Probes Inc., OR, USA, dilution 1:400). Samples were observed with the aid of an Olympus AX-70 fluorescence microscope (Olympus, Tokyo, Japan).

RT-PCR of FM-3 and FM-4 mRNA in the PVN and SON. The PVN and SON were punched out from the frozen brain slices using a method described previously [11]. Spinal cord was used as a control tissue, because it shows abundant expression of NMUR1 and NMUR2 [12]. Total RNA was extracted from the samples using Trizol reagent (Invitrogen Co., Carlsbad, CA) as described previously [13]. First-strand cDNA was synthesized from 2 μg of total RNA by random primer reverse transcription using a SuperScript III First-strand cDNA synthesis kit (Invitrogen Co.). The resulting cDNA was subjected to PCR amplification using sense and antisense primers specific for FM-3 and FM-4 by using iCycler (582BR: Bio-Rad Laboratories, Tokyo, Japan). The primer sets used for rat NMUR1and NMUR2 were as follows: rat NMUR1 primer set: 5′-C ACGACTCCCATAGCCA-3′ (sense), 5′-TCACACCCTGGATCCCT GTT-3′ (antisense); rat NMUR2 primer set: 5′-GATGAATCCCTT GAGGCGAA-3′ (sense), 5′-ATGGCAAACACGAGGACCAA-3′ (antisense). PCR products were electrophoresed on a 2% agarose gel. GAPDH was used as a control housekeeping gene, as reported previously.

Immunofluorescence double staining for AVP and Fos in the PVN and SON. Immunohistochemical staining for AVP and cFos was performed 90 min after icv injection of 0.5 nmol NMS. Frozen brain sections were cut with a cryostat at a thickness of 18 μm. The sections were pretreated with blocking solution comprising 1.5% donkey serum and 3% bovine serum albumin for 1 h, and then incubated for 2 days at 4 °C with rabbit antiserum against rat AVP (Progen Biotechnik, Inc., Heidelberg, Germany) together with goat antiserum against rat cFos (Santa Cruz Biotechnology Inc. Cal., USA). After washing, the sections were incubated with a second antibody solution comprising Alexa-488-labeled anti-rabbit IgG antibody and Alexa-546-labeled donkey anti-goat IgG antibody solution (Molecular Probes, Inc.) for 30 min, followed by observation with a fluorescence microscope (Akisoskope 2plus, Zeiss, Germany).

Statistical analysis. The data (means ± SEM) were analyzed statistically by ANOVA and Student's t test. Differences at $P < 0.05$ were considered statistically significant.

Results and discussion

Plasma AVP levels after icv injection of NMS were significantly increased at a concentration of 0.2 and 2.0 nmol compared with the saline group (Fig. 1). The increase was observed at 5 min after icv injection, and continued for

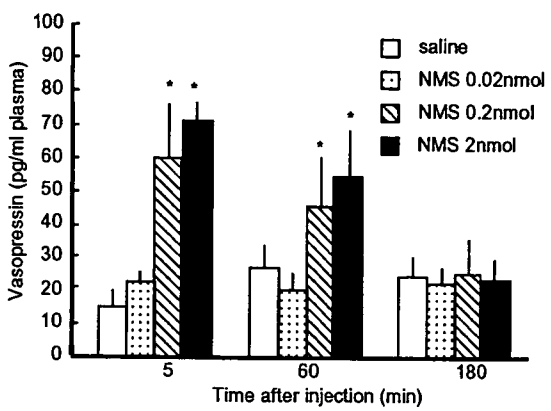

Fig. 1. Effect of icv administration of NMS on plasma AVP levels in rats. Whole blood was collected by decapitation at 5, 60, and 180 min after icv injection of 0.02, 0.2, and 2 nmol NMS or saline at 18:45 h. Each bar and vertical line represent means ± SEM ($n = 8$). Asterisks indicate significant differences from saline group ($^*P < 0.05$).

60 min. It has been shown that icv administration of neuromedin U increases the secretion of AVP, but that a very high dose (over 3 nmol) is required, and that the effect appears very slowly, with a peak at 15 and 30 min after administration [14]. Therefore, these results suggest that NMS rather than neuromedin U contributes to AVP secretion.

We then determined whether the NMS-induced increase of AVP plays a physiological role in urinary output. Icv administration of 0.2 and 2 nmol, but not 0.02 nmol, of NMS resulted in a significant decrease of urine volume during the dark period (Fig. 2A). This significant decrease did not continue until the following day (data not shown), and was unlikely to have been due to any side effect of NMS, since NMS-injected rats did not show any abnormal behavior (such as grooming, searching, attaching and barrel-rolling, which are caused by neuromedin U at doses exceeding 2 nmol). On the other hand, a larger dose of neuromedin U than that of NMS was required to cause a significant change in urinary volume, because neuromedin U at only 2 nmol caused a significant decrease (Fig. 2A). With regard to water intake, however, only a high dose of NMS caused a significant decrease during the dark period (Fig. 2B), and neuromedin U exerted no effect at any dose. These results indicate that NMS decreases urinary output during the dark period in rats, independent of water intake. The fact that a small dose (0.2 nmol) of NMS, but not neuromedin U, affected urinary output suggests that NMS has a more predominant and physiological involvement in the regulation of urinary output than neuromedin U. Although it is unclear why the NMS-induced decrease in urinary output is more potent than that of neuromedin U, both peptides bind to same receptors with similar affinity *in vitro*. However, these differences between NMS and neuromedin U are also evident in terms of their anorexic effect and their phase-shifting effect on free-running rhythm [1,5,14]. The possibility that NMS acts on another unknown receptor cannot be excluded, and further studies will be required to investigate this issue.

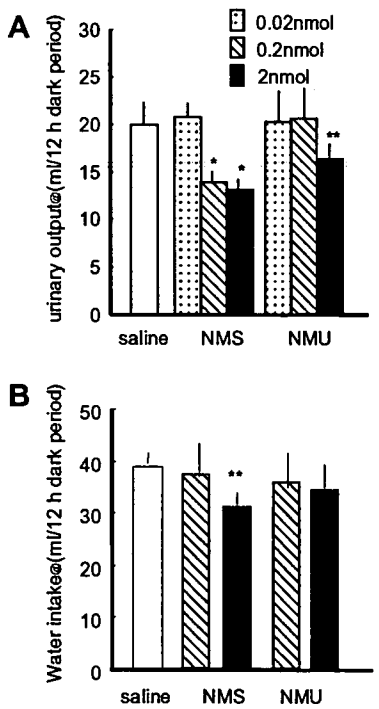

Fig. 2. Effect of icv administration of NMS on urinary output and water intake. Icv injections of saline as a control, or 0.02, 0.2, and 2 nmol of NMS and neuromedin U (NMU), were performed at 18:45 h and then urine volume (A) and water intake (B) were measured at 07:00 on the following morning. Each bar and vertical line represent means ± SEM ($n = 8$). Asterisks indicate significant differences from the saline group ($^{*}P < 0.01$, $^{**}P < 0.05$).

To evaluate the participation of NMS in AVP secretion in detail, we examined the possibility of direct action of NMS on AVP neurons in the PVN and SON. RT-PCR analysis revealed that NMUR2 mRNA, but not NMUR1 mRNA, was expressed in both the PVN and SON in rats (Fig. 3A). In comparison with mRNA expression in spinal cord, NMUR2 mRNA expression in the PVN and SON was relatively weak. Expression of GAPDH mRNA was confirmed in all tissues (data not shown). In addition, cells immunostained with antiserum against NMUR2 were also observed in the PVN and SON (Fig. 3B1 and B2).

Immunohistochemical analysis revealed that AVP-containing neurons were distributed mainly in the magnocellular region of the PVN and a wide area of the SON (Fig 3C1 and D1). In the PVN, cFos induced after icv injection of 0.2 nmol NMS was denser in the parvocellular region than in the magnocellular region (Fig. 3C2). Such cFos expression was partly observed in AVP neurons in the PVN and SON (Fig. 3C3 and D3). No effect was seen in saline-treated animals (data not shown).

We confirmed the presence of cFos expression in many neurons other than AVP neurons in the PVN and SON. In the PVN, the parvocellular region contains mainly corticotrophin releasing hormone (CRH) and AVP neurons, whereas the magnocellular region contains mainly OXT and AVP neurons [15,7]. In the SON, on the other hand, the dorsal and ventral magnocellular regions contain mainly OXT and AVP, respectively [7]. The wide expression of cFos after icv injection of NMS may indicate that NMS affects the secretion of not only AVP but also CRF and OXT. This possibility is supported by the fact that (1) NMUR2 is expressed on AVP- and OXT-containing neurons in the PVN [9], and (2) the NMS-induced anorexic effect was inhibited by a CRH antagonist, as reported previously [5].

Although the mechanism involved in the stimulation of AVP secretion by NMS is unknown, the following possibilities can be suggested. We have previously reported that the NMS mRNA expressions were observed in PVN and SON with relatively low levels [1], which may stimulate AVP secretion through a paracrine or autocrine action within these nuclei. We have also reported previously that NMS is dominantly expressed in the SCN and has a diurnal peak

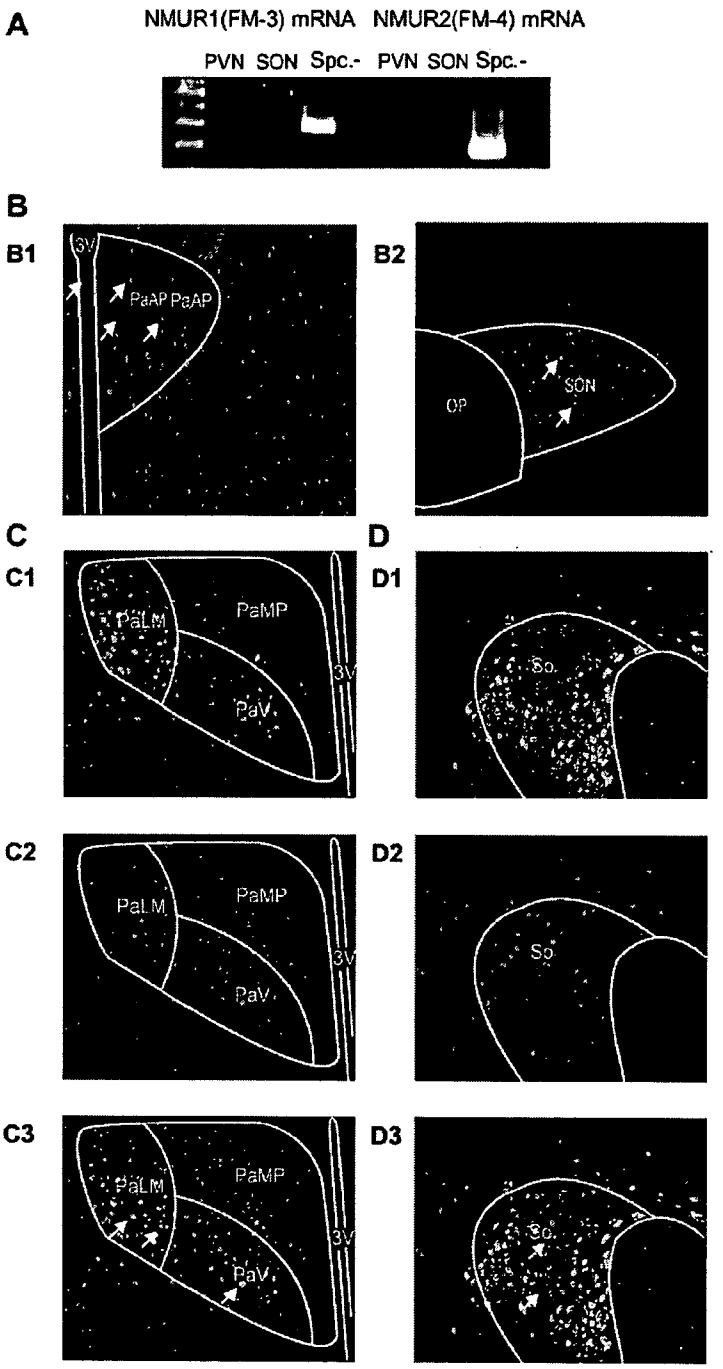

Fig. 3. (A) Expression of NMUR1 and NMUR2 mRNA in the PVN, SON, and spinal cord (Spc.). cDNA fragments from PVN and SON tissues punched out from frozen hypothalamic slices and spinal cord were amplified by PCR in the presence of oligonucleotide primers specific for NMUR1 and NMUR2. GAPDH mRNA expression was confirmed in RNA from all tissues (data not shown). (−) Indicates negative control. (B) Immunofluorescence staining for NMUR2 by anti-NMUR2 antiserum in a frozen hypothalamic slice. The area indicated by the white line in B1 and B2 shows the region of the PVN and SON, respectively. (C, D) Immunofluorescence staining for AVP in the PVN (C1) and SON (D1), and cFos expression after icv injection of 0.2 nmol NMS in the PVN (C2) and SON (D2). Dual immunostaining for cFos (red) and AVP (green) in the PVN (C3) and SON (D3). OP, optic chiasma; PaLM, paraventricular hypothalamic nucleus, lateral magnocellular part; PaV, paraventricular hypothalamic nucleus, ventral part; PaMP, paraventricular hypothalamic nucleus, medial parvicellular part; PaAP, paraventricular hypothalamic nucleus, anterior parvocellular part; 3V, third ventricle. (For interpretation of color mentioned in this figure the reader is referred to the web version of the article.)

under light/dark conditions [1]. In rats, the plasma level of AVP also shows a circadian rhythm, being high in the light period and low in the dark period. Therefore, the circadian rhythm of AVP may be reflected by NMS rhythm. If so, the rhythm of urinary output may be regulated by the rhythm of NMS in SCN. In which case, it may be specu-

lated that NMS secreted from SCN during diurnal period is transported to AVP neuron in SON and PVN through axonal projection, and shows diurnal antidiuretic action through stimulating the AVP secretion. During the nocturnal period, on the other hand, decrease of NMS from SCN may cause the decrease of AVP release and allow increasing of urinary output in rats.

In conclusion, the present findings indicate that central NMS may play an important role in urinary output through AVP secretion from the PVN and SON in rats.

Acknowledgments

We thank Y. Mori for technical assistance. This study was supported in part by the Program for Promotion of Basic Research Activities for Innovative Bioscience (PROBRAIN), Grant-in-Aid for Scientific Research(s) from the Ministry of Education, Science, Sports, and Culture of Japan (N.M), and by the Program for Promotion of Fundamental Studies in Health Sciences of the National Institute of Biomedical Innovation (NIBIO) (K.K).

References

[1] K. Mori, M. Miyazato, T. Ida, N. Murakami, R. Serino, Y. Ueta, M. Kojima, K. Kangawa, Identification of neuromedin S and its possible role in the mammalian circadian oscillator system, EMBO J. 24 (2005) 325–335.

[2] A.D. Howard, R. Wang, S.S. Pong, T.N. Mellin, A. Strack, X.M. Guan, Z. Zeng, D.L. Williams, S.D. Feighner, C.N. Nunes, B. Murphy, J.N. Stair, H. Yu, Q. Jiang, M.K. Clements, C.P. Tan, K.K. McKee, D.L. Hreniuk, T.P. McDonald, K.R. Lynch, J.F. Evans, C.P. Austin, C.T. Caskey, L.H. Van der Ploeg, Q. Liu, Identification of receptors for neuromedin U and its role in feeding, Nature 406 (2000) 70–74.

[3] R. Fuji, M. Hosoya, S. Fukusumi, Y. Kawamata, Y. Habatae, S. Hinuma, H. Onda, O. Nishimura, M. Fujino, Identification of neuromedin U as the cognate ligand of the orphan G protein-coupled receptor FM-3, J. Biol. Chem. 275 (2000) 21068–21074.

[4] M. Kojima, R. Haruno, M. Nakazato, Y. Date, N. Murakami, R. Hanada, H. Matsuo, K. Kangawa, Purification and identification of neuromedin U as an endogenous ligand for an orphan receptor GPR66 (FM3), Biochem. Biophys. Res. Commun. 276 (2000) 435–438.

[5] T. Ida, K. Mori, M. Miyazato, Y. Egi, S. Abe, K. Nakahara, M. Nishihara, K. Kanagawa, N. Murakami, Neuromedin S is a novel anorexigenic hormone, Endocrinology 146 (2005) 4217–4223.

[6] E. Vigo, J. Roa, M. López, J.M. Castellano, R. Fernandez-Fernandez, V.M. Navarro, R. Pineda, E. Aguilar, C. Diéguez, L. Pinilla, M. Tena-Sempere, Neuromedin S as novel putative regulator of luteinizing hormone secretion, Endocrinology 148 (2007) 813–823.

[7] C.H. Rhodes, J.I. Morrell, D.W. Pfaff, Immunohistochemical analysis of magnocellular elements in rat hypothalamus: distribution and numbers of cells containing neurophysin, oxytocin, and vasopressin, J. Comp. Neurol. 198 (1981) 45–64.

[8] L.W. Swanson, P.E. Sawchenko, Hypothalamic integration: organization of the paraventricular and supraoptic nuclei, Annu. Rev. Neurosci. 6 (1983) 269–324.

[9] D.L. Qiu, C.P. Chu, H. Tsukino, T. Shirasaka, H. Nakao, K. Kato, T. Kunitake, T. Katoh, H. Kannan, Neuromedin U receptor-2 mRNA and HCN channels mRNA expression in NMU-sensitive neurons in rat hypothalamic paraventricular nucleus, Neurosci. Lett. 374 (2005) 69–72.

[10] K. Nakahara, M. Nakagawa, Y. Baba, M. Sato, K. Toshinai, Y. Date, M. Nakazato, M. Kojima, M. Miyazato, H. Kaiya, H. Hosoda, K. Kangawa, N. Murakami, Maternal ghrelin plays an important role in fetal development during pregnancy, Endocrinology 147 (2006) 1333–1342.

[11] N. Murakami, K. Takahashi, Circadian rhythm of adenosine-3',5'-monophosphate content in suprachiasmatic nucleus (SCN) and ventromedial hypothalamus (VMH) in the rat, Brain Res. 276 (1983) 297–304.

[12] H. Zeng, A. Gragerov, J.G. Hohmann, M.N. Pavlova, B.A. Schimpf, H. Xu, L.J. Wu, H. Toyoda, M.G. Zhao, A.D. Rohde, G. Gragerova, R. Onrust, J.E. Bergmann, M. Zhuo, G.A. Gaitanaris, Neuromedin U receptor 2-deficient mice display differential responses in sensory perception, stress, and feeding, Mol. Cell Biol. 26 (2006) 9352–9363.

[13] K. Nakahara, R. Hanada, N. Murakami, H. Teranishi, H. Ohgusu, N. Fukushima, M. Moriyama, T. Ida, K. Kangawa, M. Kojima, The gut-brain peptide neuromedin U is involved in the mammalian circadian oscillator system, Biochem. Biophys. Res. Commun. 318 (2004) 156–161.

[14] Y. Ozaki, T. Onaka, M. Nakazato, J. Saito, K. Kanemoto, T. Matsumoto, Y. Ueta, Centrally administered neuromedin U activates neurosecretion and induction of c-fos messenger ribonucleic acid in the paraventricular and supraoptic nuclei of rat, Endocrinology 143 (2002) 4320–4329.

[15] P.E. Sawchenko, L.W. Swanson, Localization, colocalization, and plasticity of corticotropin-releasing factor immunoreactivity in rat brain, Fed. Proc. 44 (1985) 221–227.

ELSEVIER

Cardiovascular Research 76 (2007) 110–118

Cardiovascular Research

www.elsevier.com/locate/cardiores

Infusion of adrenomedullin improves acute myocarditis *via* attenuation of myocardial inflammation and edema

Bobby Yanagawa [a,1], Masaharu Kataoka [a,1], Shunsuke Ohnishi [a,*,1], Makoto Kodama [b], Koichi Tanaka [a], Yoshinori Miyahara [a], Hatsue Ishibashi-Ueda [c], Yoshifusa Aizawa [b], Kenji Kangawa [d], Noritoshi Nagaya [a,*]

[a] *Department of Regenerative Medicine and Tissue Engineering, National Cardiovascular Center Research Institute, Osaka, Japan*
[b] *Division of Cardiology, Niigata University Graduate School of Medical and Dental Sciences, Niigata, Japan*
[c] *Department of Pathology, National Cardiovascular Center, Osaka, Japan*
[d] *Department of Biochemistry, National Cardiovascular Center Research Institute, Osaka, Japan*

Received 23 January 2006; received in revised form 7 May 2007; accepted 24 May 2007
Available online 6 June 2007
Time for primary review 23 days

Abstract

Objective: Our aim was to assess whether adrenomedullin (AM), a potent vasodilator peptide with a variety of cardioprotective effects, has a therapeutic potential for the treatment of acute myocarditis in a rat model.
Methods: One week after myosin injection, rats received a continuous infusion of AM or vehicle for 2 weeks, and pathological and physiological investigations were performed.
Results: AM treatment significantly reduced the infiltration of inflammatory cells in myocarditic hearts, and decreased the expressions of macrophage chemoattractant protein-1, matrix metalloproteinase-2 and transforming growth factor-β. Myocardial edema indicated by increased heart weight to body weight ratio and wall thickness was attenuated by AM infusion (5.7±0.5 *vs.* 6.5±0.4 g/kg, and 1.9±0.3 *vs.* 2.8±0.5 mm, respectively). Infusion of AM significantly improved left ventricular maximum dP/dt and fractional shortening of myocarditic hearts (4203±640 *vs.* 3450±607 mm Hg/s, and 21.3±4.1 *vs.* 14.7±5.1%, respectively).
Conclusion: Infusion of AM improved cardiac function and pathological findings in a rat model of acute myocarditis. Thus, infusion of AM may be a potent therapeutic strategy for acute myocarditis.

Keywords: Autoimmune myocarditis; Adrenomedullin; Angiogenesis; Inflammation

1. Introduction

Acute myocarditis is a non-ischemic heart disease characterized by myocardial inflammation and edema. This disease is associated with rapidly progressive heart failure, arrhythmias and sudden death [1]. Although early evidence for efficacy of immunoglobulin and interferon therapy appears promising, these results have yet to be demonstrated in randomized or controlled clinical trials [2]. Current therapeutic options are restricted to supportive care for heart failure or arrhythmias [3]. The lack of specific treatment and the potential severity of the illness emphasize the importance of novel and effective therapeutic strategies for myocarditis.

Adrenomedullin (AM) is a potent vasodilator peptide that was originally isolated from human pheochromocytoma [4]. Earlier studies have shown that AM has beneficial hemodynamic effects on failing hearts *via* its vasodilatory action and diuretic effects [5,6]. Furthermore, AM has direct cardioprotective effects such as anti-inflammatory effects [7], inhibition

* Corresponding authors. Department of Regenerative Medicine and Tissue Engineering, National Cardiovascular Center Research Institute, 5-7-1 Fujishirodai, Suita, Osaka 565-8565, Japan. Tel.: +81 6 6833 5012; fax: +81 6 6835 5496.
E-mail addresses: sonishi@ri.ncvc.go.jp (S. Ohnishi), nnagaya@ri.ncvc.go.jp (N. Nagaya).
[1] These authors contributed equally to this work.

0008-6363/$ - see front matter © 2007 European Society of Cardiology. Published by Elsevier B.V. All rights reserved.
doi:10.1016/j.cardiores.2007.05.027